Energy and exergy analysis of SiO2/Ag-CuO plasmonic nanofluid on direct absorption parabolic solar collector

Elsevier Editorial System(tm) for Renewable Energy

Manuscript Draft

Manuscript Number: RENE-D-20-02028R2

Title: Energy and Exergy analysis of SiO2/Ag-CuO plasmonic nanofluid on direct absorption parabolic solar collector

Article Type: Research Paper

Keywords: Volumetric absorption parabolic solar collector; Binary nanofluid; Thermal efficiency; Entropy generation.

Corresponding Author: Dr. Shijo Thomas, Ph.D

Corresponding Author's Institution: National Institute of Technology, Calicut

First Author: Albin Joseph, M Tech

Order of Authors: Albin Joseph, M Tech; Sreehari Sreekumar, M Tech; Shijo Thomas, Ph.D

Abstract: Experimental investigations on the application of SiO2/Ag-CuO plasmonic nanofluid on direct/volumetric absorption parabolic solar collectors is presented in this article. The process variables for the preparation of nanofluid were optimised by employing the desirability function and response surface methodology (RSM). The optimisation was performed to achieve nanofluid with maximum possible thermal conductivity and solar absorptivity. The final solar radiation absorbed fraction and relative thermal conductivity noted for the optimised nanofluid was 82.84% and 1.234, respectively. The performance of the collector was evaluated at various flow rates from 60 lph to 90 lph, using water and optimised nanofluid as the heat transfer fluid. It is noted from the results that the thermal efficiency of the collector increases with the flow rate whereas, the exergy efficiency decreases for both water and nanofluid. The highest temperature difference of 11.27K was noted at 60lph for nanofluid which corresponds to a thermal efficiency of 57.47%. A maximum thermal efficiency of 64.05% was noted at 90 lph which corresponds to an enhancement of 48.19 % in comparison with water. Exergy efficiency of the nanofluid was enhanced by 9.4% at 60 lph, in comparison with water.

Research Data Related to this Submission

There are no linked research data sets for this submission. The following reason is given:
Data will be made available on request

Energy and Exergy analysis of SiO_2/Ag-CuO binary nanofluid on direct absorption parabolic solar collector

Albin Joseph[a], Sreehari Sreekumar[b], Shijo Thomas[a*]

[a] School of Materials Science and Engineering, National Institute of Technology, Calicut 673601, India

[b] Department of Mechanical Engineering, National Institute of Technology, Calicut 673601, India

Corresponding author:

Shijo Thomas

School of materials science and engineering

National institute of technology Calicut.

Email address: shijo@nitc.ac.in

Word count: 6072

*Cover Letter

From

Dr. Shijo Thomas
Assistant professor
School of Materials Science and Engineering
National Institute of Technology, Calicut, India

To

Editor in chief
Renewable Energy

Subject: Submission of revised manuscript for consideration towards publication.

Manuscript Number: RENE-D-20-02028R1

Respected Sir

I thank you for the valuable comments from reviewer. The manuscript has been revised as suggested. The revised **manuscript and response to the reviewers** have been uploaded for favourable consideration.

Thanking you

Yours Sincerely,

Dr. Shijo Thomas

Date: 26/09/2020
Place: NIT Calicut

Reviewer #1 (revision highlighted in yellow)

a. I have one question with regard to uncertainty calculation for the thermal, energy and exergy efficiency. I would request authors kindly give a detailed calculation for the same as response to my question.

The authors noticed a calculation and typographical error in the uncertainty section. We apologise for the same and are thankful to the reviewer for correcting us. The manuscript has been revised and have been rectified. Table 2 presents the revised uncertainties. The revision could be found in page no 10 line no 227-233.

Detailed calculation of uncertainty are presented.

1. **Heat gained or useful heat produced (W):**

Governing equation: $Q_u = m.Cp.(T_{out} - T_{in})$ (Equation no 3 in the manuscript)

Uncertainty of Eq 3 is given by

$$\frac{\sigma Qu}{Qu} = \sqrt{\left(\frac{\sigma m}{m}\right)^2 + \left(\frac{\sigma T_{in}}{T_{in}}\right)^2 + \left(\frac{\sigma T_{out}}{T_{out}}\right)^2}$$

where

$\sigma m = 0.000625\frac{kg}{sec}$, $\sigma T_{in}, \sigma T_{out} = 0.1^oC$, $Qu = 883.05W$, $m = 0.025\frac{kg}{sec}, T_{in} = 30^oC$, $T_{in} = 38.41^oC$,

Hence

$$\frac{\sigma Qu}{Qu} = \sqrt{(0.025)^2 + (0.0033)^2 + (0.0026)^2} = \pm 2.53\%$$

2. **Thermal efficiency**

Governing equation: $\eta_{th} = m.Cp.(T_{out} - T_{in})/(A.I)$ (Equation no 6 in the manuscript)

Uncertainty of Eq 6 is given by

$$\frac{\sigma \eta_{th}}{\eta_{th}} = \sqrt{\left(\frac{\sigma m}{m}\right)^2 + \left(\frac{\sigma T_{in}}{T_{in}}\right)^2 + \left(\frac{\sigma T_{out}}{T_{out}}\right)^2 + \left(\frac{\sigma I}{I}\right)^2}$$

Where

$$\sigma m = 0.000625 \frac{kg}{sec}, \qquad \sigma T_{in}, \sigma T_{out} = 0.1^{o}C, \qquad \sigma I = 5 \frac{W}{m^2}, \qquad I = 850 \frac{W}{m^2}$$

Hence

$$\frac{\sigma \eta_{th}}{\eta_{th}} = \sqrt{(0.025)^2 + (0.0033)^2 + (0.0026)^2 + (0.0058)^2} = \pm 2.60\%$$

3. Exergy efficiency

Governing equation: $\eta_{Ex} = 1 - \frac{T_{amb} \times S_{gen}}{\left[1 - \frac{T_{amb}}{T_{sun}}\right] Q_s}$ (Equation no 10 in the manuscript)

Uncertainty of Eq 10 is given by

$$\frac{\sigma \eta_{Ex}}{\eta_{Ex}} = \sqrt{\left(\frac{\sigma m}{m}\right)^2 + \left(\frac{\sigma T_{in}}{T_{in}}\right)^2 + \left(\frac{\sigma T_{out}}{T_{out}}\right)^2 + \left(\frac{\sigma T_{amb}}{T_{amb}}\right)^2 + \left(\frac{\sigma I}{I}\right)^2}$$

Where

$$\sigma m = 0.000625 \frac{kg}{sec}, \qquad \sigma T_{in}, \sigma T_{out}, \sigma T_{amb} = 0.1^{o}C, \qquad \sigma I = 5 \frac{W}{m^2}, \qquad \sigma T_{amb} = 32^{o}C,$$

Hence

$$\frac{\sigma \eta_{Ex}}{\eta_{Ex}} = \sqrt{(0.025)^2 + (0.0033)^2 + (0.0026)^2 + (0.0031)^2 + (0.0058)^2} = \pm 2.62\%$$

Table. 2: Uncertainties of variables

Variables	Uncertainty
Flow rate	≤± 2.5 %
Solar irradiance	≤ ± 5.00 W/m^2
Heat Gained	≤ ± 2.53 %
Thermal efficiency	≤ ± 2.6 %
Exergy efficiency	≤ ± 2.62 %

b. I hope the parabolic concentrator will heat the fluid at-least to a temperature >100 degree celsius. Why authors presented the variation in thermal conductivity only in a low temperature range?

We agree with the reviewers comment. However in the present study the maximum temperature achieved was nearly 50^{o}C. Due to this reason the variation in thermal conductivity was analysed till 50^{o}C.

Highlights

- Influence of SiO_2/Ag-CuO nanofluid on direct absorption parabolic collector.
- Exergy and energy analysis was performed at various flow rate
- A maximum thermal efficiency of 64.12 % was noted at 90 lph.
- Exergy efficiency decreased with flow rate whereas thermal efficiency increased.

Energy and Exergy analysis of SiO_2/Ag-CuO plasmonic nanofluid on direct absorption parabolic solar collector

Albin Joseph[a], Sreehari Sreekumar[b], Shijo Thomas[a*]

[a] School of Materials Science and Engineering, National Institute of Technology, Calicut 673601, India

[b] Department of Mechanical Engineering, National Institute of Technology, Calicut 673601, India

Corresponding Author: Shijo Thomas, Email Address: shijo@nitc.ac.in

ABSTRACT

Experimental investigations on the application of SiO_2/Ag-CuO plasmonic nanofluid on direct/volumetric absorption parabolic solar collectors is presented in this article. The process variables for the preparation of nanofluid were optimised by employing the desirability function and response surface methodology (RSM). The optimisation was performed to achieve nanofluid with maximum possible thermal conductivity and solar absorptivity. The final solar radiation absorbed fraction and relative thermal conductivity noted for the optimised nanofluid was 82.84% and 1.234, respectively. The performance of the collector was evaluated at various flow rates from 60 lph to 90 lph, using water and optimised nanofluid as the heat transfer fluid. It is noted from the results that the thermal efficiency of the collector increases with the flow rate whereas, the exergy efficiency decreases for both water and nanofluid. The highest temperature difference of 11.27K was noted at 60lph for nanofluid which corresponds to a thermal efficiency of 57.47%. A maximum thermal efficiency of 64.05% was noted at 90 lph which corresponds to an enhancement of 48.19 % in comparison with water. Exergy efficiency of the nanofluid was enhanced by 9.4% at 60 lph, in comparison with water.

Keywords: Volumetric absorption parabolic solar collector, Binary nanofluid, Response surface methodology, Thermal efficiency, Entropy generation.

Nomenclature

.A	Area of parabola (m^2)	T_{in}	Inlet temperature (K)
A_p	Aperture width of parabola(m)	T_{sun}	Temperature of Sun (K)
C_p	Specific heat of working fluid (kJ/kg.K)	θ	Rim angle of the parabola
		σ	Uncertainty
E_{des}	Energy destruction (W)	τ_t	Transmittance of absorber tube
f	Focal length of the parabola (m)	r_r	Reflectivity of reflector
I	Solar irradiance (W/m^2)	η_{ex}	Exergy efficiency
m	mass flow rate (kg/sec)	η_{th}	Thermal efficiency
Q_u	Heat gained (W)	η_{opt}	Optical efficiency of the parabola
Q_s	Available direct solar energy (W)	RSM	Response surface methodology
Q_o	Energy loss (W)	RTC	Relative thermal conductivity
S_{gen}	Entropy generation (W/K)	SRAF	Solar radiation absorbed fraction
T_{amb}	Ambient temperature (K)	S1	Entropy generated during the transfer of heat to working fluid from solar irradiance
T_{out}	Outlet temperature (K)	S2	Entropy generated during the heat loss

1. Introduction

The persistent consumption of fossil fuels made them insufficient to meet the overwhelmingly increasing demand of energy. Stepping up the utilisation of sustainable energy sources is a widely acknowledged optimistic solution to meet the ever augmenting need for energy. Solar energy, a potential replacement to fossil fuels, provides high hope to overcome the energy crisis to a certain extent, especially in electricity generation and various heating application [1]. Solar energy being a sustainable and clean source of energy is gaining widespread attention for many thermal applications. A number of studies have been reported based on the solar energy conversions like solar thermal conversion, photo electric conversion and photo electric thermal conversion. The solar thermal convertors like dish collector, linear Fresnel reflectors (LFR) and parabolic trough collector (PTC) are the most preferred techniques for the medium and high temperature applications. In these techniques solar radiation is concentrated to a line or a point from which it is transferred to the working fluid (heat transfer fluid). Parabolic collectors are widely used for solar thermal application due to its better performance and comparative cost effectiveness. A parabolic trough collector is equipped with three components mainly, the parabolic reflector plate equipped with an absorber tube at its focal point and the working fluid inside the absorber tube. In a

typical operation of parabolic collector, solar ray is concentrated (using a parabolic reflector) towards the receiver tube placed at the focal line of the reflector, from which the converted energy in the form of heat is transferred by a working fluid for various applications like water heating, space heating, solar refrigeration system and even for power generation [2]. The solar thermal collectors could be coupled with various thermal systems like power generators, in order to improve the efficiency of the whole unit. Bakos and Tsechelidou [3] investigated solar trough collector coupled with the lignite fired steam power plant using a TRNSYS simulation software. They found that the Rankine efficiency of the plant improved from 33% to 37.64%. They also claim that the solar power plant could reduce the total fuel consumption and thus the CO_2 emission.

Apart from the design parameters of the parabolic collector, researchers now a days are focusing on the modification of absorber tubes. Solar absorptivity of the absorber tube is an important parameter that influences the performance of the collector [4, 23]. The absorber tube is an intermediate between the solar radiation and the working fluid. The absorption of solar energy will heat up the absorber tube. This heat is then conducted from the outer surface to the inner surface of the absorber tube which then is transferred to the heat transfer fluid/working fluid through convection. The intermediate heat losses through convection and radiation from the hot absorber tube surface to ambient, results in a deterioration in the performance of the collector [5, 22, 24]. This is where the concept of direct/volumetric absorption solar collectors gains significance by significantly reducing the thermal losses since the photo thermal conversion is directly achieved by the heat transfer fluid/working fluid [6]. Solar radiation absorption capability of the working fluid is the metric of performance of the volumetric absorption solar thermal conversion systems. The poor solar absorptivity of commonly used working fluids like deionised water, ethylene glycol, thermal oils, etc. renders them unfit for direct application in direct absorption collectors. Improving the solar absorptivity of these fluids is an area of active research [7, 8].

Nanofluids, with enhanced optical properties, are a suitable replacement for conventional heat transfer fluid in volumetric absorption solar collectors. Qin,et al. [9] made a performance evaluation of novel volumetric solar absorption parabolic collector using plasmonic nanofluids with constant absorption coefficient. An additional reflective coating was given on the upper half of the receiver tube that enhances the optical path length and investigations were performed by varying the receiver tube diameter. They concluded that thermal efficiency of the collector reduced with the diameter and at optimal diameter the direct absorption collector exhibit better performance than the conventional collectors. The

authors also claim that direct absorption parabolic collectors are effective at low flowrate ($\leq$0.18kg/s). As per the reports of Bhalla et al. [10] a layer of silicon envelope over the nanofluids could reduce the thermal losses due to convection to the atmosphere. The enhancement on temperature was nearly 3.5^{o}C. Wang et al. [11] introduced a novel technique which improved the efficiency of the direct absorption collector by introducing reverse irradiation. As per their observation the temperature within the fluid was almost uniform compared to the directed irradiated system, which establishes the influence of the nanoparticles in the fluid. However, the enhancement in the properties of nanofluid is limited up to a critical concentration, beyond which the properties of the nanofluid drops. The reason is attributed to reduced stability of the nanofluid at higher concentrations due to the agglomeration and sedimentation of the nanoparticles [28]. Recent reports [12] reveals that binary nanofluids exhibits better properties as compared to conventional nanofluids, due to the combined effect of two or more particles [13]. Bhalla at al. [14] investigated the influence of Al_2O_3/Co_3O_4 binary nanofluid on direct solar absorption system and compared it with that of the surface absorption system. The authors noticed 5.4^{o}C rise in the temperature for optimum direct absorption fluid compared to the surface absorption system. The reports of Chen et al. [15] reveals that improved optical properties are noted for binary nanofluid in which a broad absorption of solar radiation was observed. Zeng and Xuan [16] reports that the plasmonic effect of noble nanoparticles exhibits high photo thermal conversion. SiO_2/Ag is one of the commonly used plasmonic nanoparticles. However, the hybrid nanoparticles are found to be larger in size due to which the stability of the nanofluid is affected highly. As per the reports of Keblinski et al. [17] the particles size have very high impact on stability and properties of the nanofluid. The improved effectiveness of the nanofluid is observed at lower particle size. Thermo-optical properties of the nanofluid have very high significance in the direct absorption solar collector [29, 30]. Due to this reason it is highly recommended to employ working fluid with high thermal and optical properties in volumetric absorption solar collectors. From these perspectives, it is clear that the binary nanofluid in which more than one nanoparticles are dispersed, is capable to achieve both. The colloidal stability of the nanoparticles in the fluid is one of the main practical drawback associated with nanofluids. Nevertheless, this issue can be addressed by various methods like addition of surfactants, varying pH of the fluid, surface functionalization of the nanoparticles, etc. By enhancing the mutual repulsion between the particles, the chance of agglomeration of the particles and further sedimentation can be prevented. Zeta potential analysis is one of the method used to quantify the colloidal stability of nanofluids. An absolute value of zeta potential greater the

30 mv is considered to yield a stable nanofluid. However, for flow applications the issue of the stability is less pronounced since the fluid under circulation is in continuous agitation [18].

In the present study the performance evaluation of the volumetric absorption collector using plasmonic SiO_2/Ag-CuO binary nanofluid is investigated experimentally. Additional advantages on photo-thermal conversion of nanofluid could be observed in SiO_2/Ag particles due to the plasmonic effect, the thermal transport within the nanofluid is being influenced by the CuO nanoparticles. The desirability function combined with the response surface methodology (RSM), a widely adopted technique in industries for multi objective response process, was used to optimise the process variables involved in the study [19, 20]. The experiments were conducted at National Institute of Technology Calicut (latitude: 11.3216, longitude: 75.9336). Thermo-optical properties exhibited by the nanofluid as well as the collector efficiency and entropy generation of the collector are analysed using the optimised SiO_2/Ag-CuO nanofluid, and compared with base fluid. Even though many lab scale studies on the optical properties of plasmonic nanofluid were reported, to the best of the author's knowledge this is the first attempt that investigates the influence of a plasmonic binary nanofluid on a volumetric absorption parabolic collector.

2. Materials and methods

2.1 Synthesis of SiO_2/Ag-CuO nanofluid.

SiO_2/Ag-CuO nanofluid was synthesised by two step method in which the particles are added and dispersed in the water. SiO_2/Ag particle used in the fluid was prepared by introducing Ag on the SiO_2 by reducing $AgNO_3$ with $SnCl_2$. CuO nanoparticles used are directly purchased from Sigma Aldrich. To achieve a stable suspension, sodium dodecyl sulfonate was used as surfactant. Optimisation of the concentration of nanoparticle and surfactant were done using a desirability function. The detailed procedure of synthesis of nanofluid and optimisation is mentioned in the earlier investigation conducted by the same authors [28]. The optimised nanofluid is then used in the volumetric absorption solar collector.

2.2. Design and manufacturing of experimental setup.

2.2.1 Parabolic reflector

The length of parabolic trough is 1500 mm and the aperture width is 1080 mm. Three troughs of dimensions 500 mm length and 1080mm aperture diameter each were fabricated using the glass wool - epoxy composite. Anodised aluminium sheets were used as the reflector. The reflector sheets were fixed on the glass wool-epoxy composite parabolic trough so that the reflector attain the parabolic trough shape. The rim angle of the parabola is 90^o and Eq. 1 represents the parabolic profile of the fabricated trough.

$$Y = 0.925X^2 \quad (1)$$

The focal point of the parabola is given by equation 2

$$f = \frac{Ap}{2} Cot\theta + \frac{Ap^2}{16\, f} \quad (2)$$

Where f is focal length of the parabola, θ is the rim angle and A_p, the aperture width of the parabola.

The dimensions of the parabolic trough are presented in Table 1.

Table. 1: Dimension of parabolic trough fabricated.

Parameter	**Dimension**
Length of parabola	1.5 m
Distance of focal point	0.272 m
Aperture width	1.05m
Aperture Area	1.575 m^2
Rim angle	90^o
Outer tube inner diameter	0.035 m
Inner tube inner diameter	0.015 m

2.2.2 Absorber Tube.

Optical absorptivity and other dimensions of the absorber tube highly influences the thermal and optical efficiency of a parabolic solar collector. In the present system, glass-glass absorber tube made of quartz is used, which enable high transmittance, reducing the optical losses of absorber tube. Moreover, the evacuation of glass- glass annulus could reduce the convective heat losses [10]. A provision was made on the experimental setup to adjust the position of the absorber tube so as to maintain the absorber tube exactly at the focal point of

the parabolic trough. Both ends of the absorber tube were sealed using Teflon coupling which could withstand temperature up to 350^{o}C and high temperature RTV silicon (anabond) was used as sealant.

2.2.3 Solar Tracker

Continuous tracking of sun is mandatory for the collector to get perpendicular rays on its surface. To accomplish this a solar tracker was employed. The tracker consist of a geared motor which is connected to the axis of parabolic collector. The sun tracking was achieved using an LDR photo resister as the sensor. The LDR sensor unit (not clear in the figure due to its small size) placed on the trough is connected to geared motor unit with an intermediate PCB circuit.

2.2.4 Experimental procedure.

The parabolic trough collector used in the present study is located at National Institute of Technology, Calicut in the North-South direction (latitude: 11.3216, longitude: 75.9336). The experiment was carried out on clear sunny days during the month of March and April. The hydraulic cycle chosen for the study is shown in Fig 1. According to Fig 1 the nanofluid from a reservoir is pumped to the parabolic collector and then to a heat exchanging unit (constant temperature bath). The heat exchanger cools the nanofluid and maintain a constant temperature at the inlet of absorber tube. The nanofluid from the heat exchanger is finally directed to the reservoir. The flow rate of the nanofluid was varied using a valve and flow meter. The inlet and outlet temperatures were noted using calibrated T-type thermocouples, connected to a data logger (Agilent). The temperatures were noted at every 5 minutes interval from 09:45 am to 4:15 pm and average temperature for every 30 minutes were determined.

As mentioned in Section 2.2 the nanofluid was synthesised based on the range of concentration mentioned in Table 3 and its thermo-optical properties were measured. An optimised process variables of nanofluids were achieved that enables maximum possible solar radiation absorption and thermal conductivity. The nanofluid prepared using this optimised combination is further experimentally analysed to quantify its effect on volumetric absorption parabolic collector (VAPC). The influence of this nanofluid on VAPC at various flow rates starting from 60 lph to 90 lph, were analysed and compared with that of base fluid.

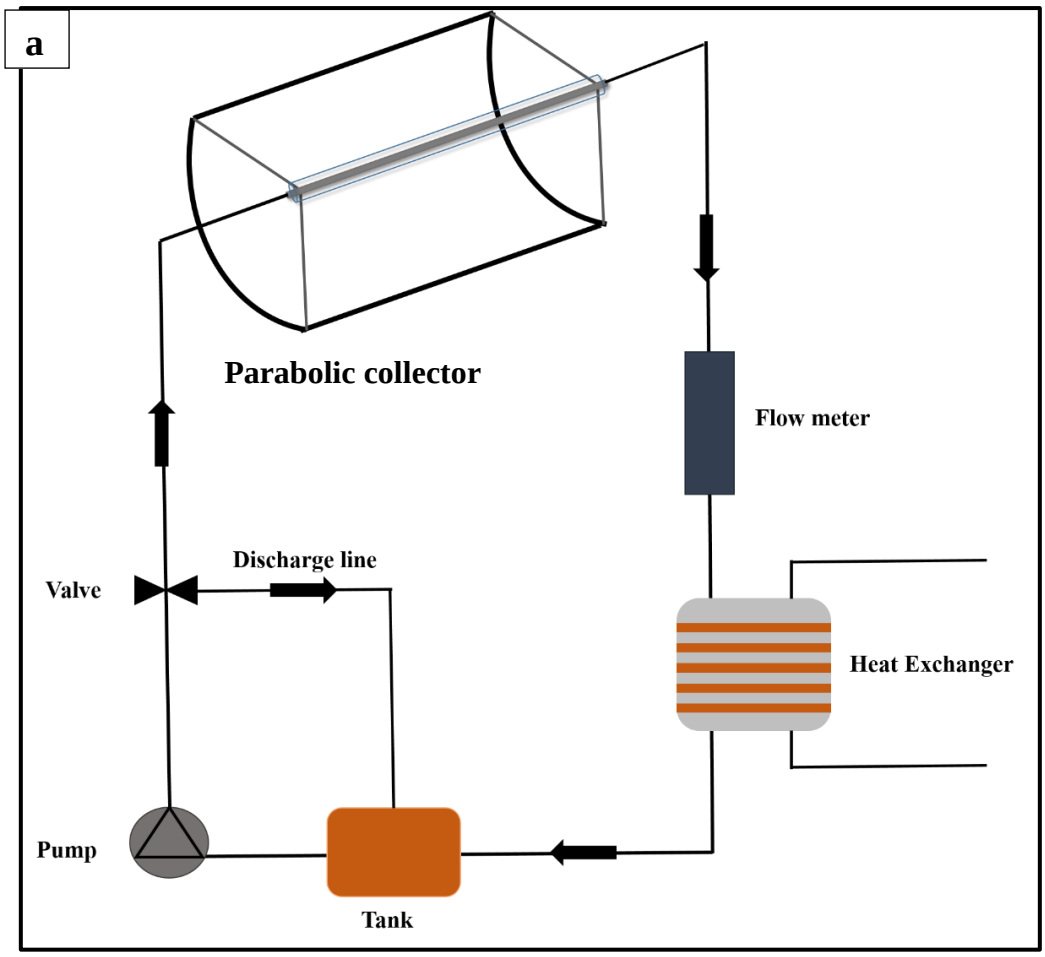

197

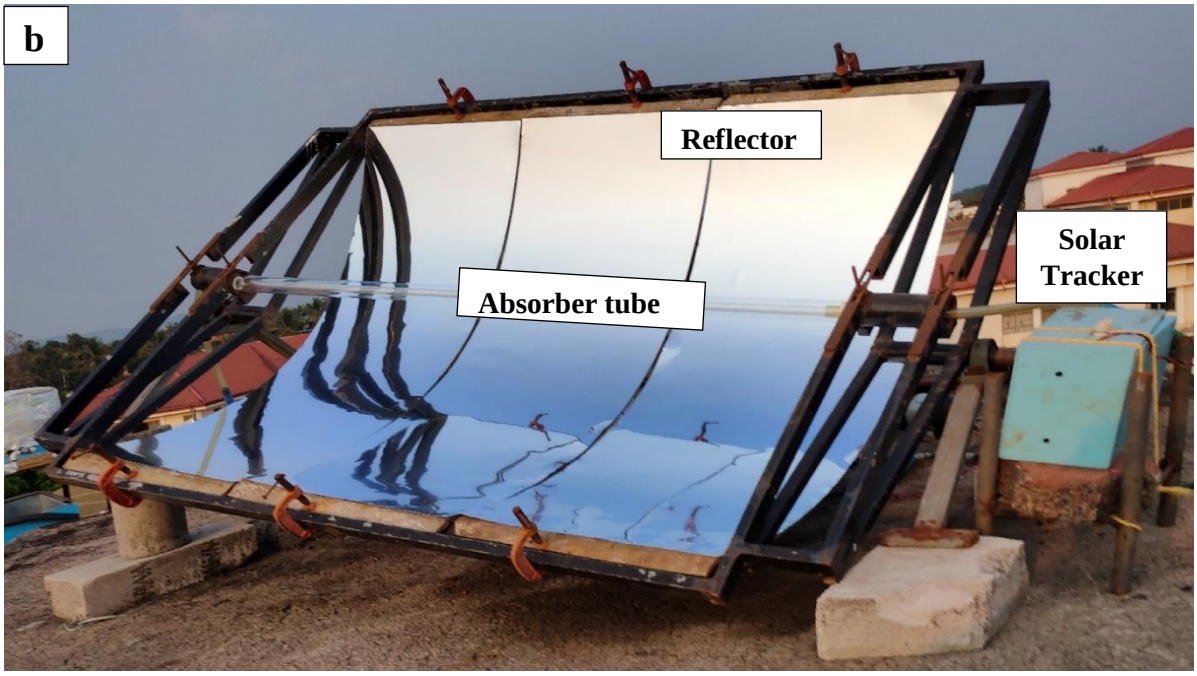

198

199 Fig. 1. a) Schematic of experimental setup, b) Photograph of fabricated parabolic trough

200

2.3 Mathematical formulation

Mathematical formulation used for the estimation of performance parameters are listed below:

Useful heat produced (W):

$$Q_u = m.Cp.(T_{out} - T_{in}) \quad (3)$$

Available direct solar energy:

$$Q_s = A.I \quad (4)$$

Optical and thermal efficiency of the parabola was calculated using equation 5 and 6

$$\eta_{opt} = \tau_t r_r \quad (5)$$

$$\eta_{th} = \frac{Q_u}{Q_s} \quad (6)$$

Entropy generation (W/K):

$$S_{gen} = mCp\ ln(\frac{T_{out}}{T_{in}}) - \frac{Q_s}{T_{Sun}} + \frac{Q_o}{T_{amb}} \quad (7)$$

The entropy generation during the heat transfer from sun to nanofluid and inside absorber tube was estimated using Eq 7. The entropy generated due to the pressure drop during fluid flow is neglected as it was insignificant.

$$Q_o = Q_s - mC_p\ (T_{out} - T_{in}) \quad (8)$$

Energy destruction (W):

$$E_{des} = S_{gen} \times T_{amb} \quad (9)$$

Exergy efficiency:

$$\eta_{Ex} = 1 - \frac{T_{amb} \times S_{gen}}{\left[1 - \frac{T_{amb}}{T_{sun}}\right] Q_s} \quad (10)$$

2.4 Experimental Uncertainty Analysis

The uncertainty experimental data was estimated using the method descried by Moffat [26]. Table 2 presents the estimated uncertainty of various parameters. The calibration of thermocouple was done by employing a constant temperature bath as standard. The maximum error in the thermocouple was found to be ± 0.1K, the uncertainty of Heat gained, thermal and exergy efficiency was calculated from the equation 11-13

$$\frac{\sigma Qu}{Qu} = \sqrt{\left(\frac{\sigma m}{m}\right)^2 + \left(\frac{\sigma T_{in}}{T_{in}}\right)^2 + \left(\frac{\sigma T_{out}}{T_{out}}\right)^2} \quad (11)$$

$$\frac{\sigma \eta_{th}}{\eta_{th}} = \sqrt{\left(\frac{\sigma m}{m}\right)^2 + \left(\frac{\sigma T_{in}}{T_{in}}\right)^2 + \left(\frac{\sigma T_{out}}{T_{out}}\right)^2 + \left(\frac{\sigma I}{I}\right)^2} \quad (12)$$

$$\frac{\sigma \eta_{Ex}}{\eta_{Ex}} = \sqrt{\left(\frac{\sigma m}{m}\right)^2 + \left(\frac{\sigma T_{in}}{T_{in}}\right)^2 + \left(\frac{\sigma T_{out}}{T_{out}}\right)^2 + \left(\frac{\sigma T_{amb}}{T_{amb}}\right)^2 + \left(\frac{\sigma I}{I}\right)^2} \quad (13)$$

Table. 2: Uncertainties of variables

Variables	Uncertainty
Flow rate	≤± 2.5 %
Solar irradiance	≤ ± 5.00 W/m^2
Heat Gained	≤ ± 2.53 %
Thermal efficiency	≤ ± 2.6 %
Exergy efficiency	≤ ± 2.62 %

3. Result and discussion

3.1 Characterisation of nanofluids

Characterisation was limited to measurement of solar absorptivity and thermal conductivity of nanofluid and morphological analysis of nanoparticles. Data obtained from the UV-vis spectrometer (Avantes) was used to estimate the solar radiation absorbed fraction (SRAF). To quantify the thermal conductivity exhibited by the nanofluids, a thermal properties analyser (KD2 pro) was employed. Morphology of the nanoparticles were analysed using the field emission scanning electron microscope (Hitachi SU 6600) and are presented in Fig 2.

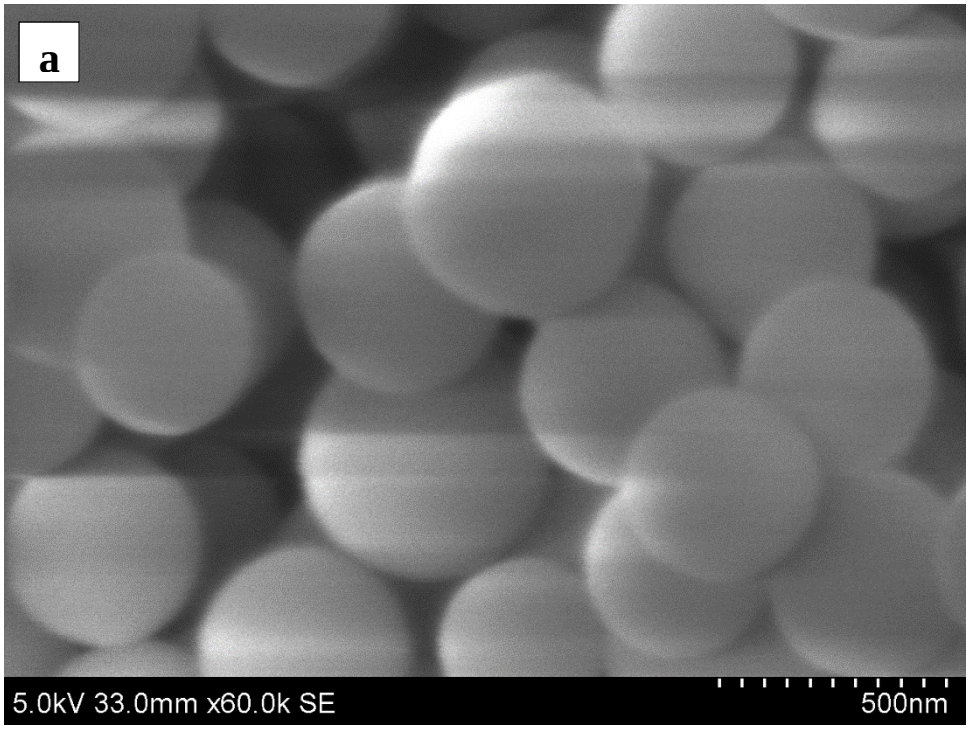

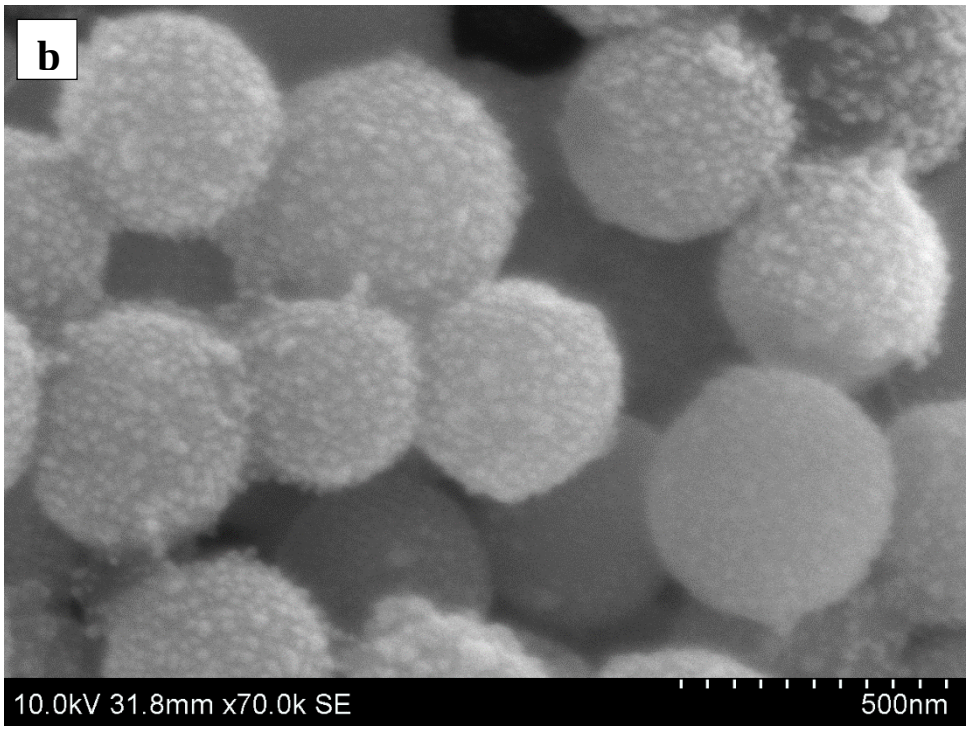

Fig. 2. SEM images a) SiO_2, b) SiO_2/Ag nanoparticles.

3.2 Optimisation of SiO_2/Ag-CuO plasmonic binary nanofluid

The optimisation of the nanofluid is detailed in the earlier publication by the same authors [28]. Desirability approach on RSM was adopted to optimise the process variables involved in the synthesis of nanofluid. Desirability function is a widely adopted approaches

to optimise multi objective problems [20]. The regression equation for relative thermal conductivity and SRAF obtained from the central composite design of response surface methodology (Eq. 14 and 15) was taken for the desirability approach [28]. The objective of the optimisation was to maximise SRAF and thermal conductivity of the nanofluids. In this approach the variables such as mass of nanoparticles like SiO_2/Ag and CuO, surfactant are in the design range (between upper limit and lower limit), while the responses like thermal conductivity and SRAF are set to be maximal. Table 3 presents the goal, lower and upper limit and importance of each process variables. The optimal combination of process variables was obtained as 206.3 mg of SiO_2/Ag per litre of DI water and correspondingly, 864.7 and 1996.2 mg of CuO and SDS respectively. Figure 3 shows the variation of desirability with change in concentration of particles. It can be seen that, the desirability drops after concentration of SiO_2/Ag particles exceeds 206.3 mg/l, which might be due to the fact that beyond this concentration the stability of the nanofluid decreases resulting in a decrease in thermal conductivity and SRAF. However, the desirability increased with the concentration of CuO and then drops after 864.7mg/l. This could be due to the fact that, as the CuO concentration increases the thermo-optical properties are found to be increased and after a critical concentration the stability of the nanofluid was affected, thus decreasing the desirability. Moreover, the stability was found to be increased with surfactant concentration due to which the desirability increases with the concentration of surfactant. The optimised concentrations of nanoparticles were found to be stable with a zeta potential of -38.7mV. The RTC and SRAF for the optimised concentration were found to be 1.234 and 82.84% respectively from the response equations. To confirm this experimentally, the optimised nanofluid combination was prepared and the experimental value of RTC and SRAF were obtained as 1.231 and 81.79% respectively. Since the predicted and experimental values are comparable to each other in addition with the desirability value of one, the results are reliable. The final optimised nanofluid is then taken to the parabolic collector for the analysis of photo thermal conversion and entropy generation. In addition thermal conductivity of the optimised nanofluid in the temperature range, 30^{o}C to 50^{o}C, was measured and presented in the Table 4. The relative thermal conductivity (Thermal conductivity of nanofluid by thermal conductivity of water) was also estimated.

.

$$RTC = 1.11825 + (4.64016\times10^{-005} \times C) + (8.23773\times10^{-006} \times B) - (7.08371\times10^{-005} \times A) - (2.81400\times10^{-008} \times A \times B) + (7.00727\times10^{-008} \times B \times C) - (1.48865\times10^{-008} \times A \times C) -$$

283 $(1.87837x10^{-008} \times C^2) - (6.43326x10^{-009} \times B^2) + (3.11178x10^{-008} \times A^2)$

284 (14)

285 SRAF = 35.2379 + (0.039759 x C) + (0.010745 x B) + (0.021866 x A) - (3.34793E-006 x A

286 x B) – (6.48624 $x10^{-006}$ x B x C) - (6.67764 $x10^{-006}$ x A x C) - (7.30303 $x10^{-006}$ x C^2) -

287 (1.95099 $x10^{-006}$ x B^2) - (1.08898 $x10^{-005}$ x A^2)

288 (15)

289 Where A, B, and C are mass of SiO_2/Ag, CuO and SDS respectively per litre of DI water.

290

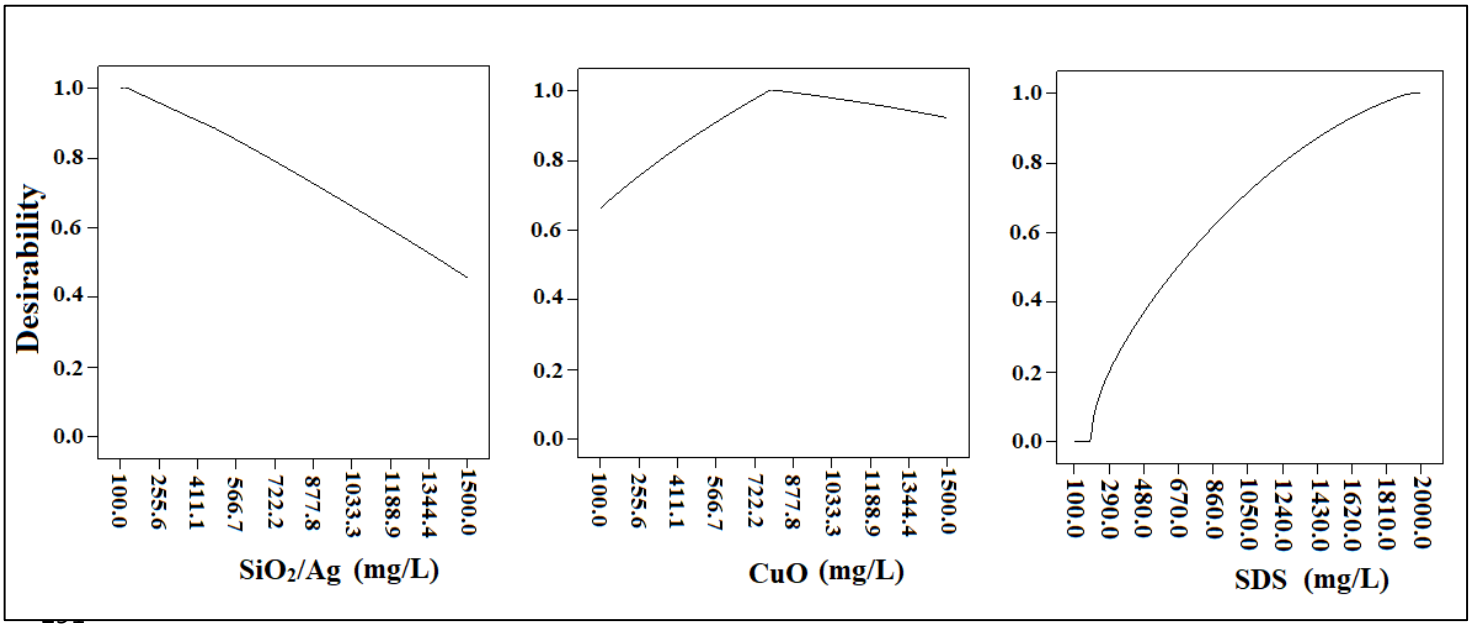

292 **Fig .3.** Variation of desirability function with process variables.

293 **Table. 3:** Conditions adopted during the optimisation.

Name	Goal	Lower limit	Upper limit	Importance
Concentration of SiO_2/Ag (mg/l)	In range	100	1500	4
Concentration of CuO (mg/l)	In range	100	1500	4
Concentration of SDS (mg/l)	In range	100	2000	4

294

295

Table 4. Thermal conductivity at various temperature

Temperature (^oC)	Relative thermal conductivity	Thermal conductivity (W/mK)
30	1.234	0.7404
35	1.248	0.7491
40	1.262	0.7576
45	1.299	0.7794
50	1.314	0.7886

3.3 Performance of SiO_2/Ag-CuO hybrid plasmonic nanofluid on parabolic collector.

The SiO_2/Ag-CuO nanofluid used as working fluid in the parabolic collector was prepared based on the optimum process variables achieved from the procedure mentioned in 3.2. The optimised valued of mass of particles and surfactant (process variables for preparing the nanofluid) are 206.3 mg/L, 864.7mg/L and 1996.2mg/L of SiO_2/Ag, CuO and SDS respectively. The experiment was carried out on a sunny day during the month of March and April. The Average solar radiation in the experimental location was 850 W/m^2. The maximum radiation noted was 950W/m^2 which mostly occur during 12:00 pm to 2:00 pm.

Figure 4 presents the temperature profile of nanofluid and the base fluid at various flow rates. The temperatures were noted from 10:00 am to 4:00 pm. As the figure says the temperature difference decreases with the increase in flow rate of working fluid. A maximum temperature difference of 11.27K was noted for the optimum nanofluid at the flow rate of 60 lph and 8.4K at 90 lph. The highest noted temperature difference for water was 2.61K, at 60lph. Table 4 shows the maximum temperature difference obtained for SiO_2/Ag-CuO nanofluid and water at various flow rates. It is apparent that the introduction of nanoparticles enhanced the performance of the collector by improving the optical and thermal properties of the nanofluid. The improved solar absorptivity of the nanofluid increased the solar thermal conversion of the collector and the enhancement in thermal conductivity augmented the heat transfer for nanofluids. The experiments were repeated three times and the reported values are the average, to ensure the repeatability. The variation of temperature difference with solar radiation is plotted and added in the manuscript as Figure 5. As can be seen form the figure the temperature difference increases with the solar radiation for a particular flow rate and the variation is almost linear. At a flow rate of 60 lph, the maximum temperature difference obtained was 10.8 ^oC for 930 W/m^2. The minimum temperature difference observed at this flow rate was 5.16 ^oC at a solar radiation of 720 W/m^2. The maximum temperature noted at 90 lph was 8.41 ^oC at 930 W/m^2 for which the maximum efficiency was also obtained. The

maximum observed temperatures were 10.21 ^{o}C and 8.96 ^{o}C at flow rates of 70 and 80 lph respectively for a solar radiation of 930 W/m^2

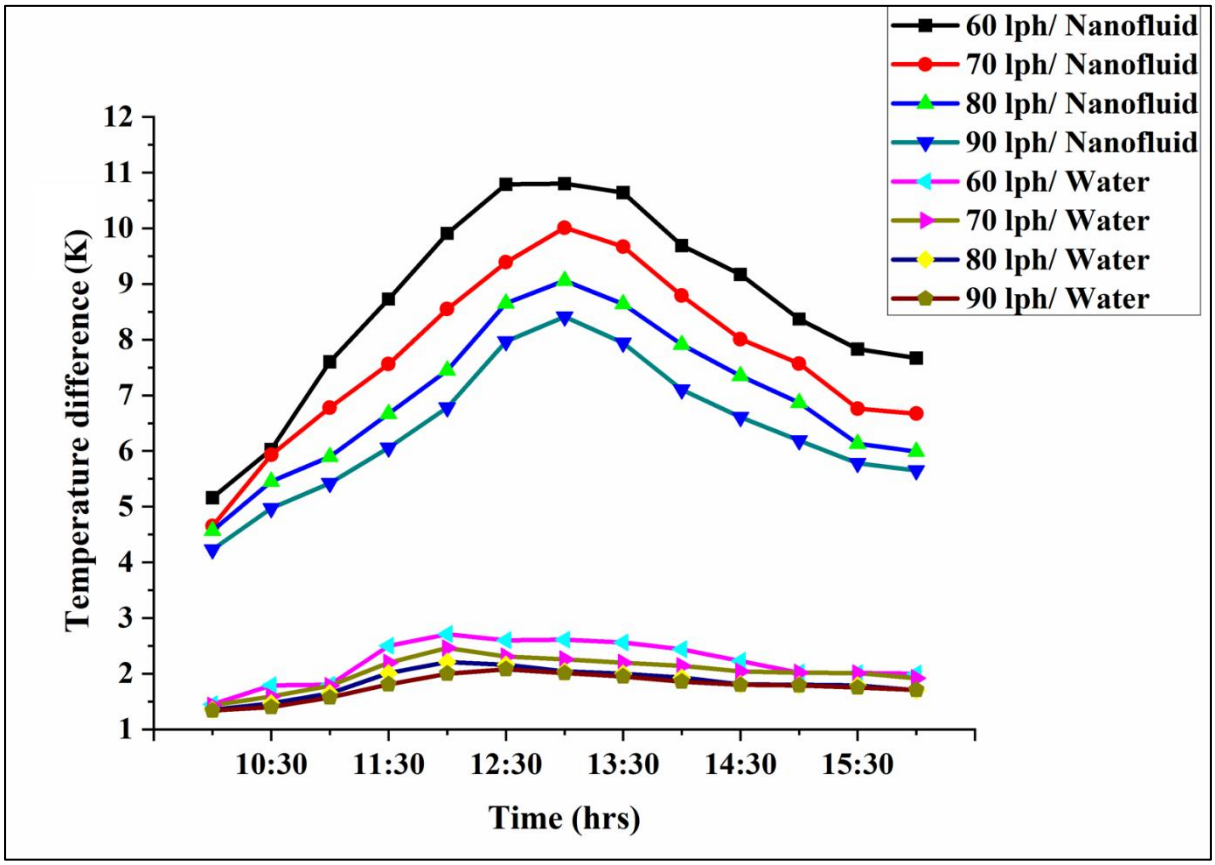

Fig. 4. Temperature profile of nanofluid and water at various flow rates.

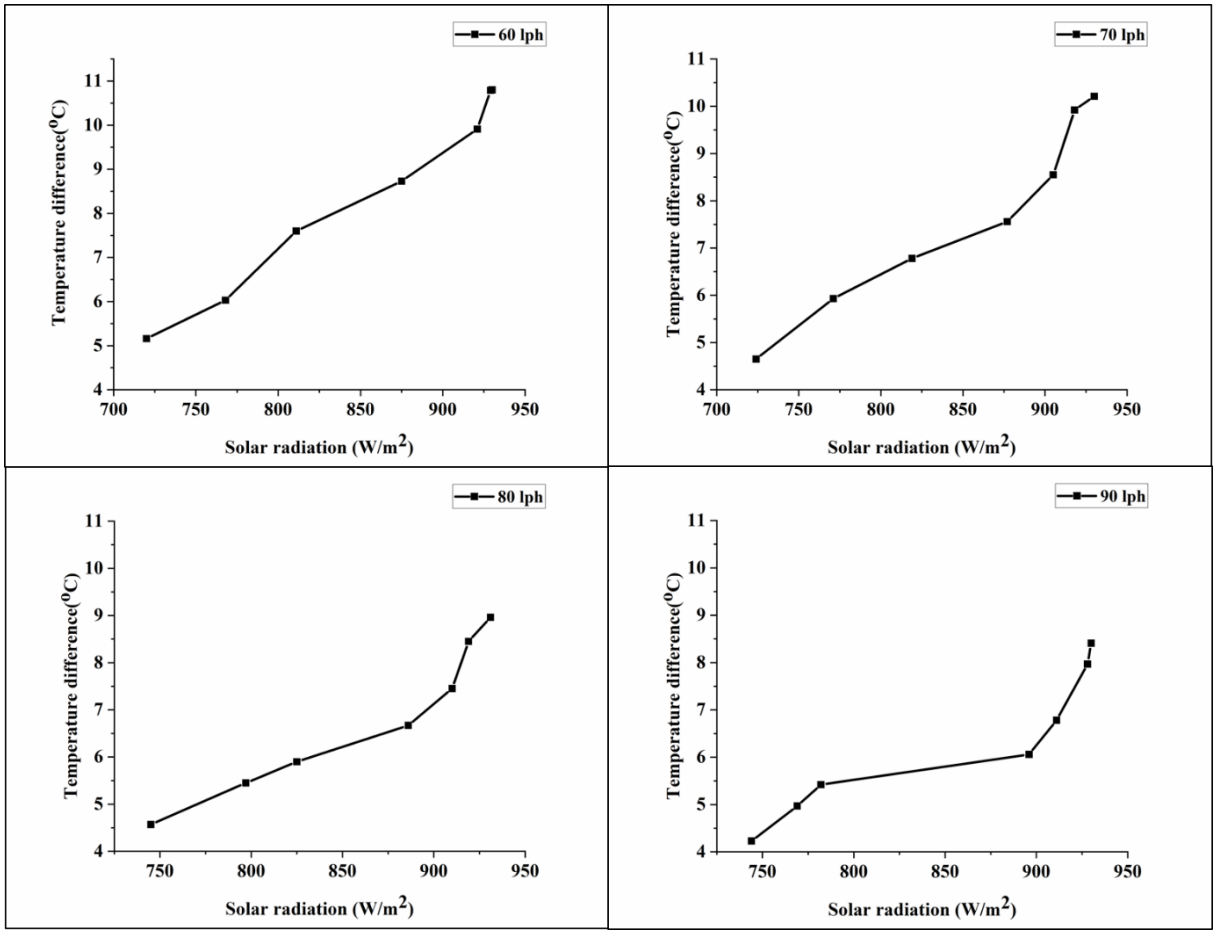

328

329 **Fig. 5** Variation of temperature difference with radiation.

330

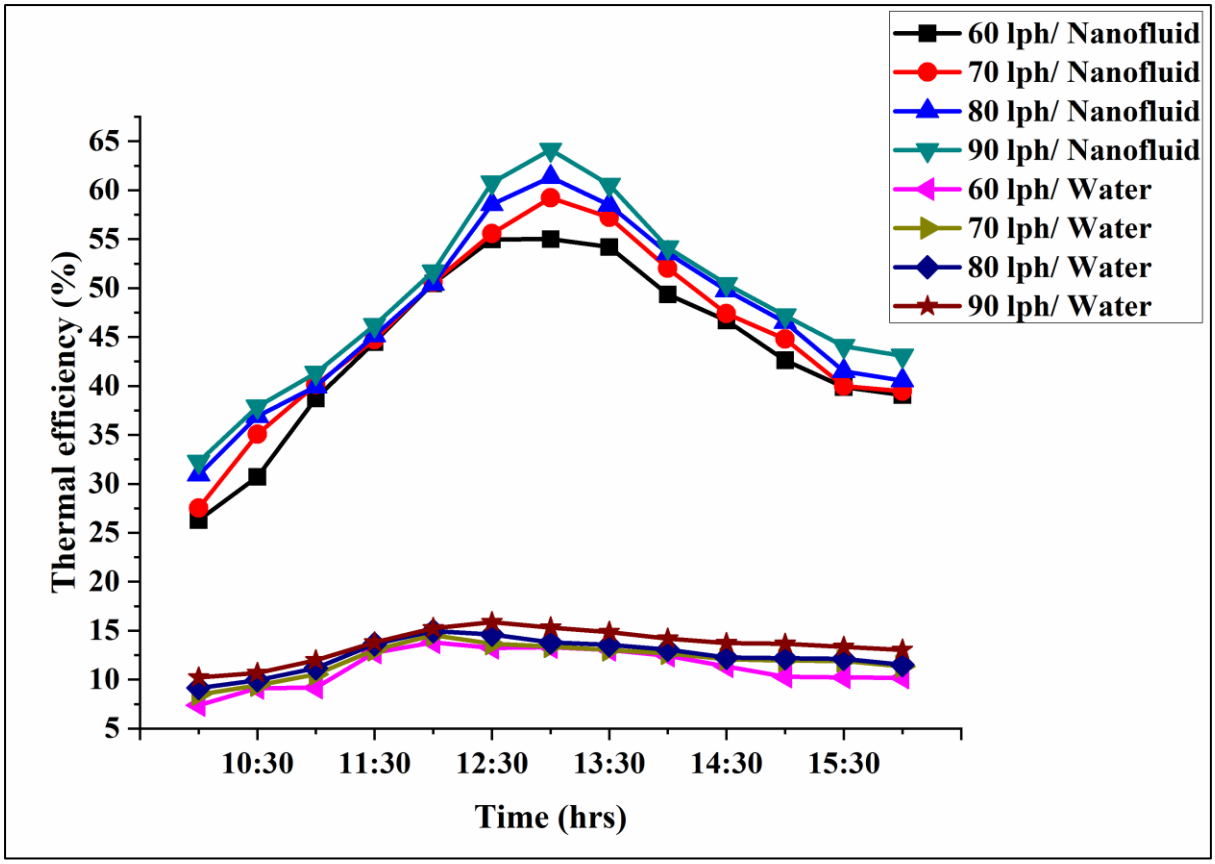

Fig. 6. Thermal efficiency plot of nanofluid and water at various flow rates.

The thermal efficiency of the collector was estimated using the equations 3, 4, 5 and 6. The transient variation of collector efficiency at various flow rate are shown in Fig. 6. The direct solar irradiance is 850 W/m^2, which is the estimated average solar radiation at the location. The maximum thermal efficiencies for water are 13.29, 14.55, 14.96 and 15.86% at flow rates of 60, 70, 80 and 90 lph, respectively. The corresponding values of efficiencies estimated for nanofluid are 57.40, 60.41, 63.72 and 64.13% respectively. In addition, it could be observed from Fig. 6 that the maximum efficiency was obtained during the time period of 12:00 pm to 2:00 pm. As mentioned before, the efficiency of the collector depends on the thermo-optical properties of the working fluid. Plasmonic SiO_2/Ag nanoparticles used in the present investigation exhibited an additional improvement in the optical absorptivity of the fluid which in turn resulted in better photo thermal conversion. It is reported that in comparison with other nanoparticles plasmonic nanoparticles exhibit an additional self-heating due to the plasmonic effect, which in turn enhance the photo thermal conversion efficiency of the nanofluid [16, 21]. The presence of CuO in the fluid transfers the absorbed

348 solar energy effectively, which is attributed to its higher thermal conductivity [17]. Reynolds
349 number is another parameter that influences the efficiency of the collector. The heat transfer
350 becomes more effective as the Reynolds number/ flow rate increases which also results in the
351 increased efficiency of the collector [25, 31]. As explained in equation (6) thermal efficiency
352 of the collector is defined as the ratio of useful heat produced to the available direct solar
353 energy. As the flow rate increases the amount of useful heat carried away by the working
354 fluid increases. As the flowrate increases the local mixing between the fluid and solid
355 particles and also between the fluid and the tube surface increases which results in enhanced
356 thermal transport and reduced thermal loss [32].

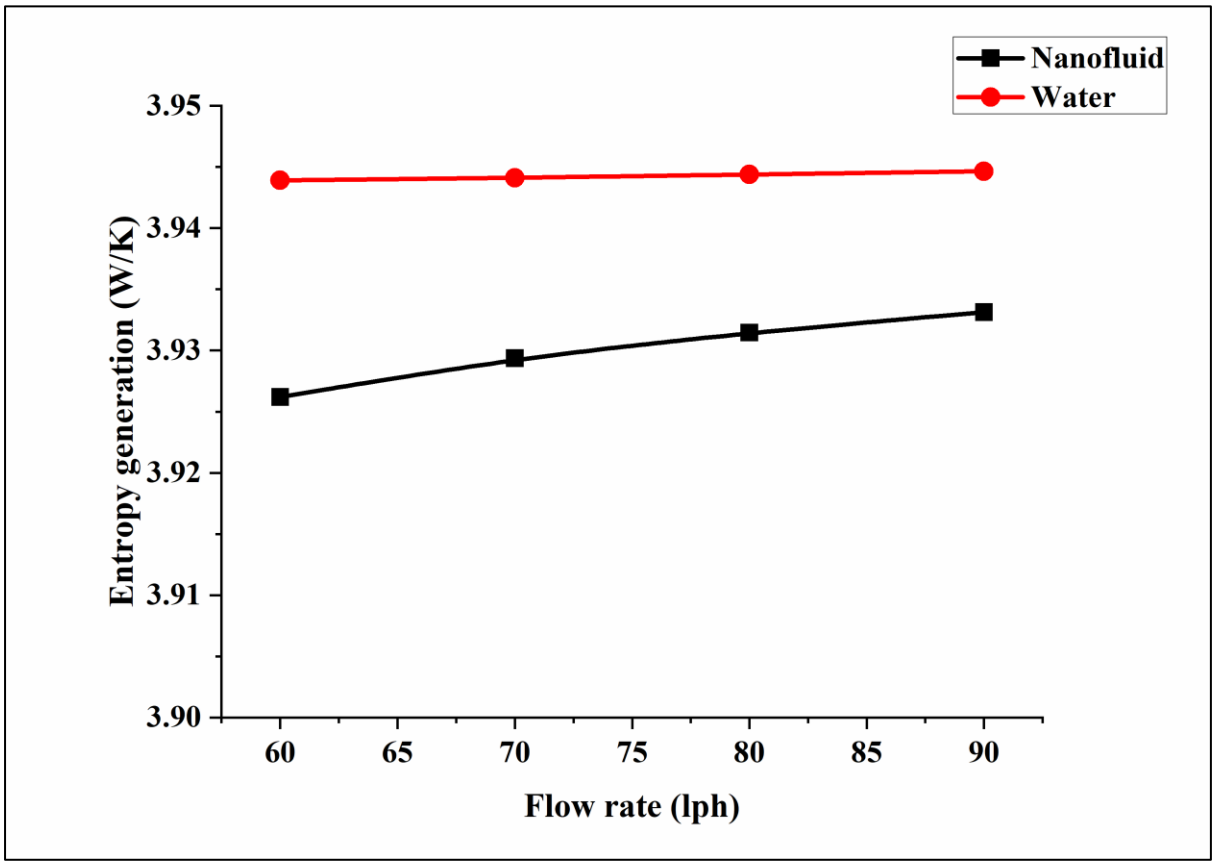

357

358 **Fig. 7.** Average entropy generation at various flowrates.

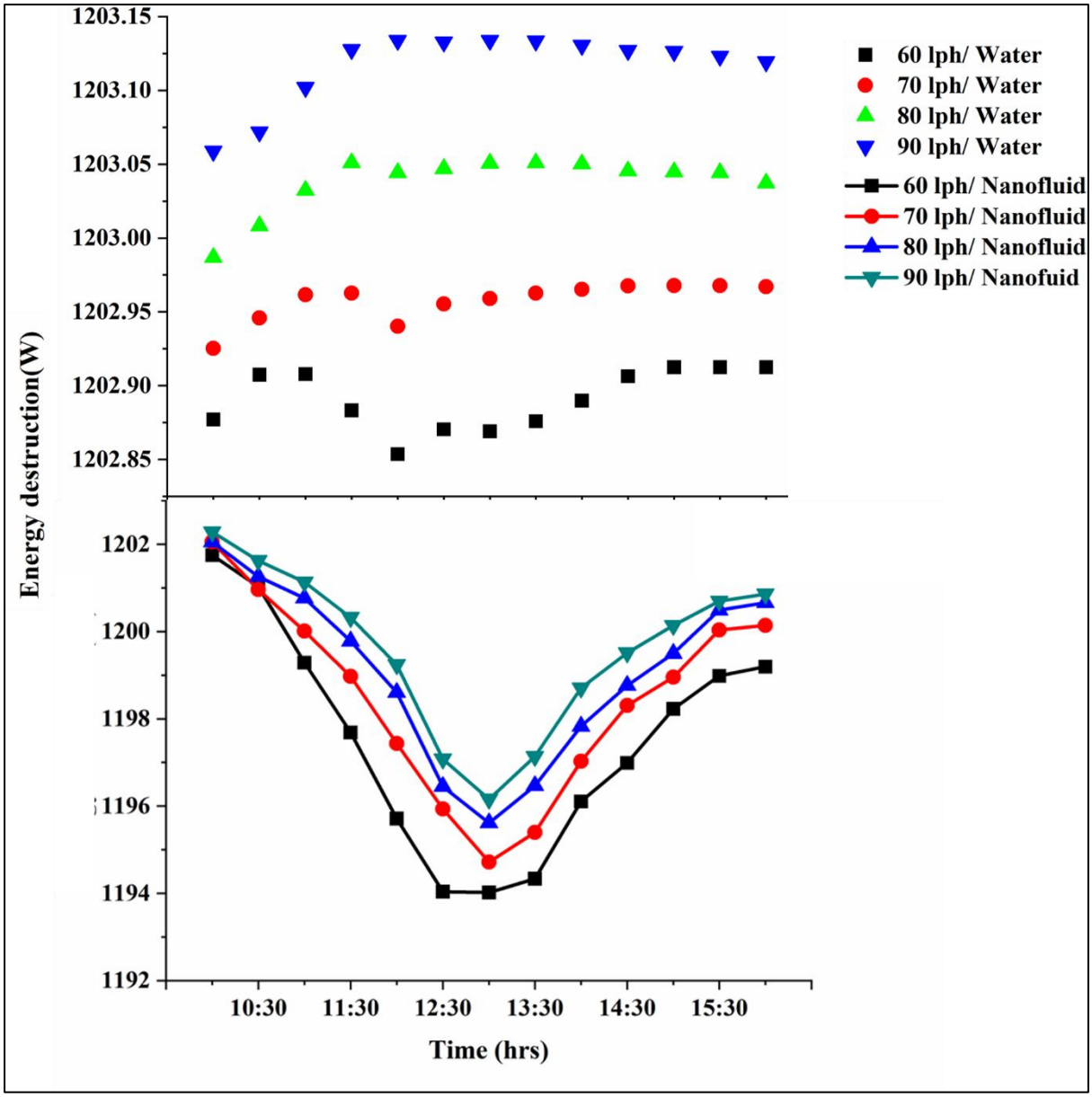

Fig. 8. Energy destruction profile of nanofluid and water at various flowrates.

Figures 7 and 8 shows the entropy generation and energy destruction calculated using equations 7, 8, 9 and 10. As can be seen from Figure 7, the entropy generation slightly decreased with the dispersion of nanoparticles in water. The entropy generation was almost constant with change in flow rate in the case of water, while it slightly increased with flowrate for nanofluid. In the present study, two factors could be accounted for the entropy generation. 1) Entropy generation due to the heat transfer from solar irradiance to the nanofluid (S1). 2) Entropy generated during to the heat loss from the nanofluid to the surroundings (S2). The contribution of the two sources (S1 & S2) to entropy generation in water and nanofluids at different flow rates is shown in Fig. 9. Among these two sources, the

entropy generation due to the heating up of the nanofluid as it flows through the collector tube from inlet to outlet (S1) was found to be lesser than the entropy generation due the heat losses from the nanofluid (S2). At a flowrate of 90 lph the S1 for water was 72.14% lower than that of nanofluid. The S1 for water was found to be less compared to nanofluid since the heat gain was less in water when compared to nanofluid. However, entropy generated due to the losses (S2) was found to be less compared to water and reduces with the flow rate for nanofluids. At a flowrate of 90 lph the S2 for water is 81.54% higher than that of nanofluid. The contribution of entropy generation due to heat losses (S2) of water being much higher than that of nanofluid is the reason for the slight increase in overall entropy generation (S1+S2) of water with flow rate. On comparing figures 10 and 11 with Fig. 4 it can be seen that, at a particular flow rate S1 increases with temperature difference whereas S2 decreases (Fig 10 and 11). The higher absorption of heat by the plasmonic nanofluids results in higher temperature gain of the fluid and thus contributes to S1. In spite of the high temperature rise of the fluid the heat losses to the ambient is lesser in volumetric absorption systems employing plasmonic nanofluids is evident from the decreasing S2 values. The variation of thermal efficiency and exergy efficiency with the flow rate is presented in Fig 12. It can be seen that in the case of the optimised nanofluid, the exergy efficiency shows a slight decrease with flow rate, while thermal efficiency increases. But the exergy efficiency of the nanofluid was found to be higher than that of water with an enhancement of 9.4% at 60 lph. It could be surmised that the energy losses associated with the volumetric absorption system reduces with the flow rate while employing nanofluid, while the generated entropy during the gain of heat from the sun increases with the flow rate. The increase in overall generation of entropy is attributed to the development of temperature drop between the top wall of the collector and the outlet due to the enhanced heat gain [27]. In addition, unlike the surface absorption based parabolic collector, in volumetric absorption solar collector the working fluid directly absorbs and convert the solar irradiance. Since the absorbing medium is in a kinematic state, the flow rate directly affects the conversion of solar energy to heat. At higher flow rate of working fluid, the energy conversion might be incomplete due to the insufficient time available for the energy absorption owing to the rapid motion of nanoparticles in the working fluid.

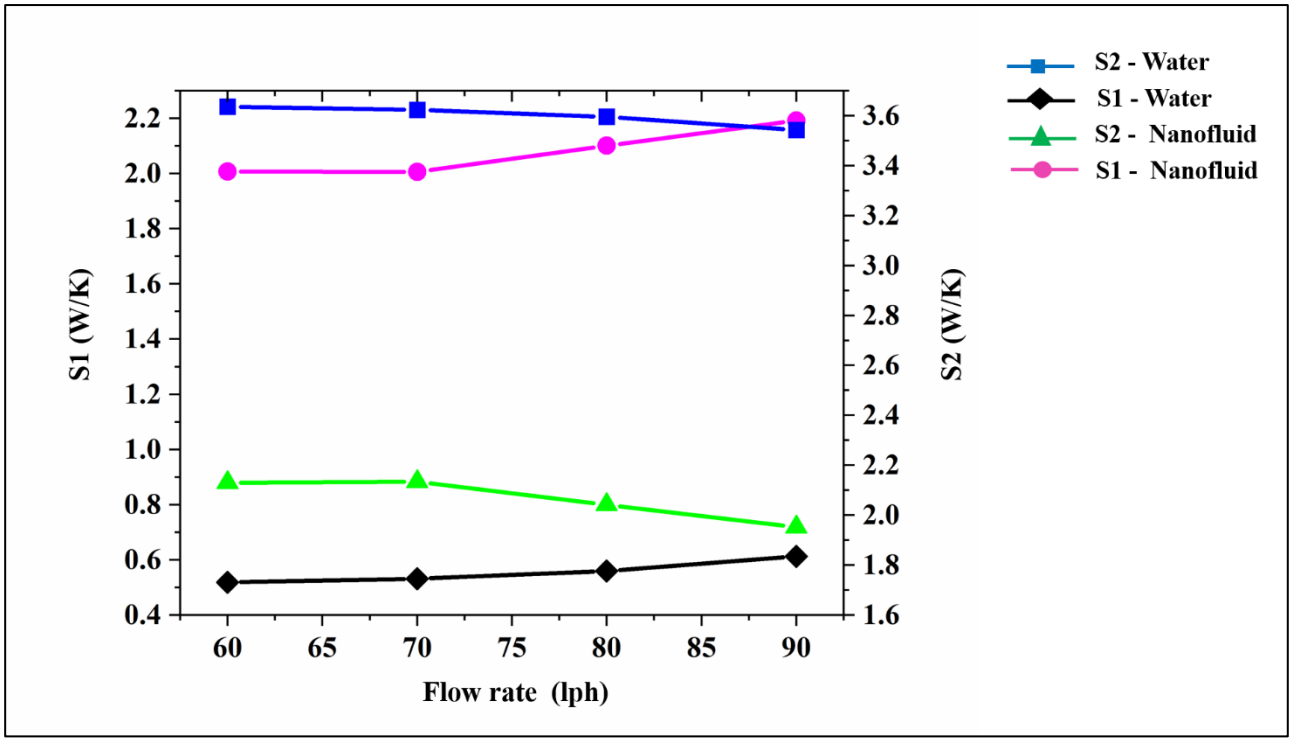

399

400 **Fig. 9**. Variation of average S1 and S2 with various flowrate.

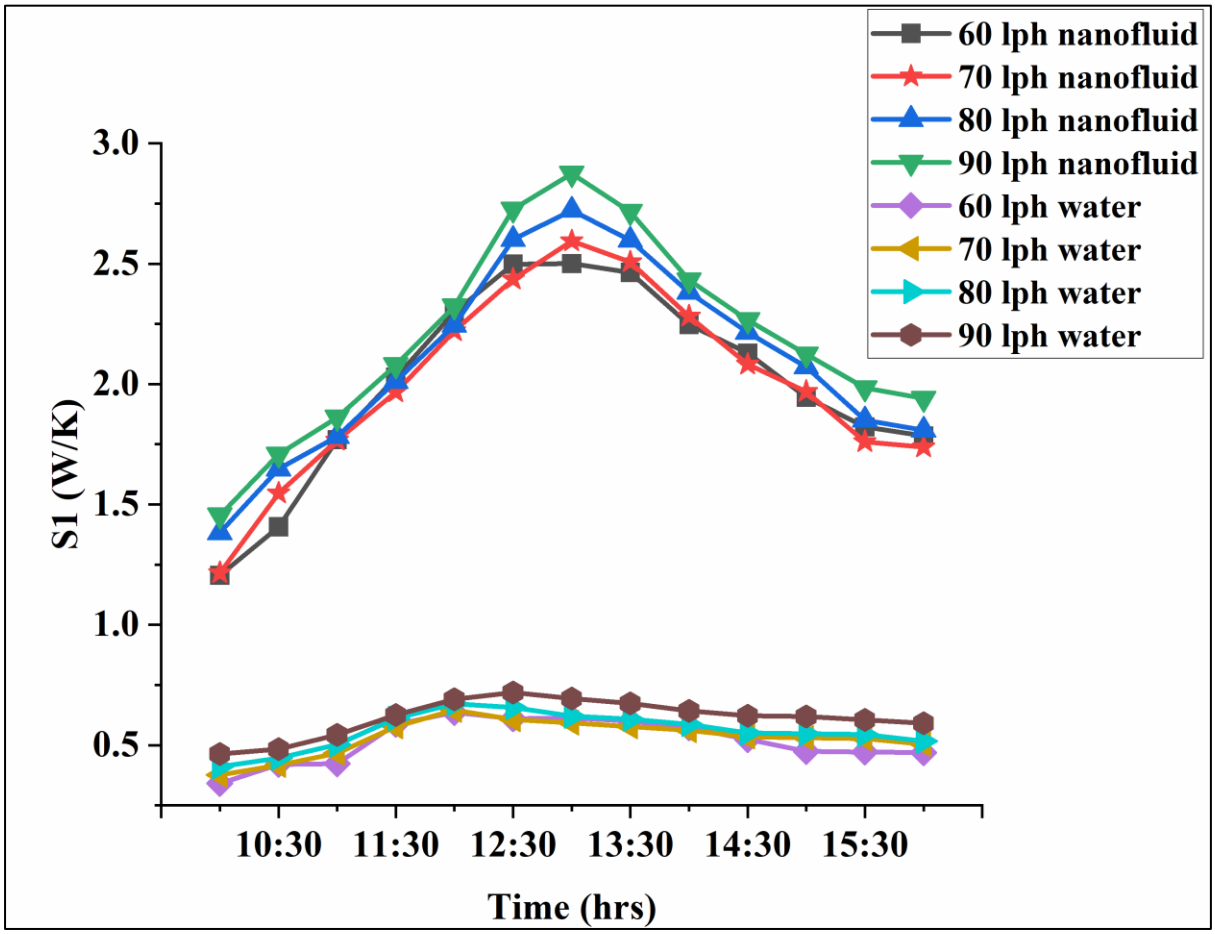

401

402 **Fig.10**: Instantaneous S1 of nanofluid and water at various flow rates.

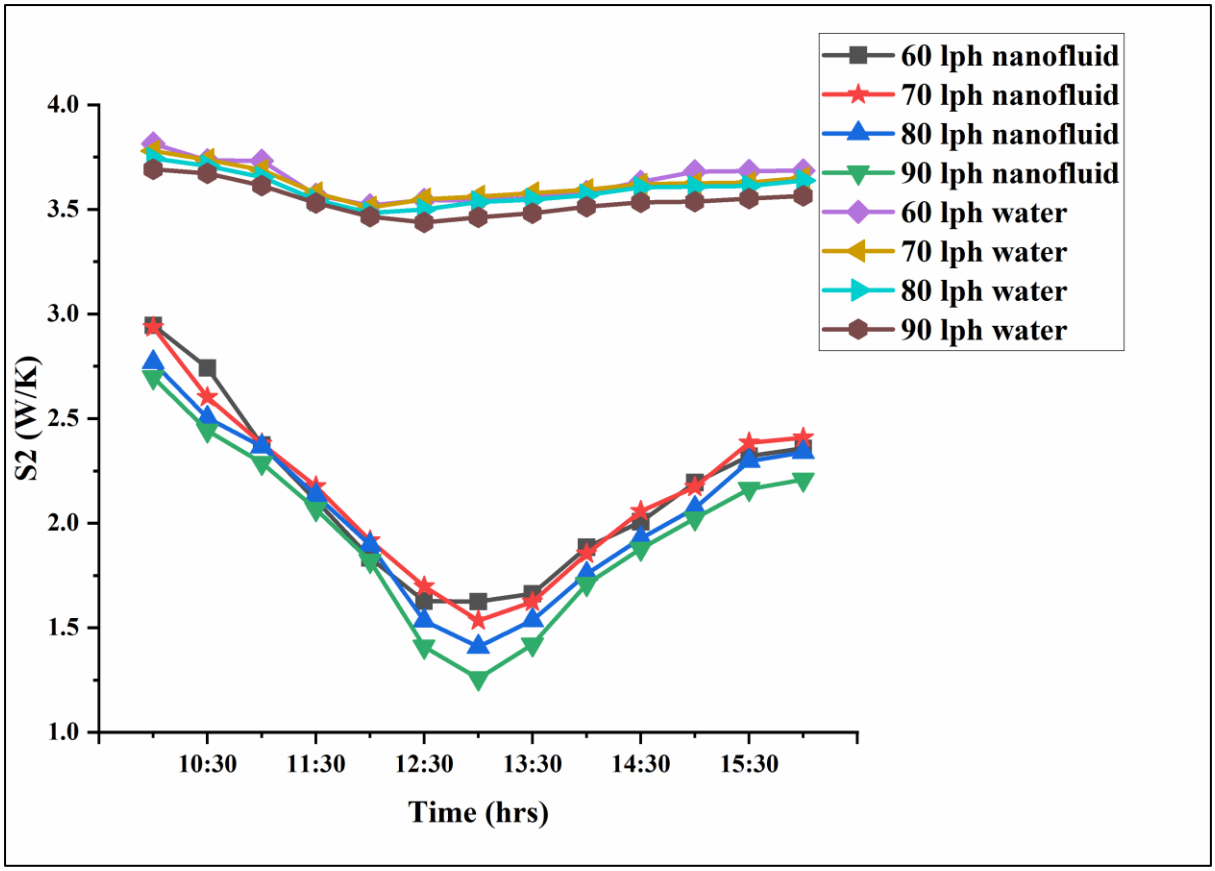

403

404 **Fig. 11**. Instantaneous S2 of nanofluid and water at various flow rates.

405

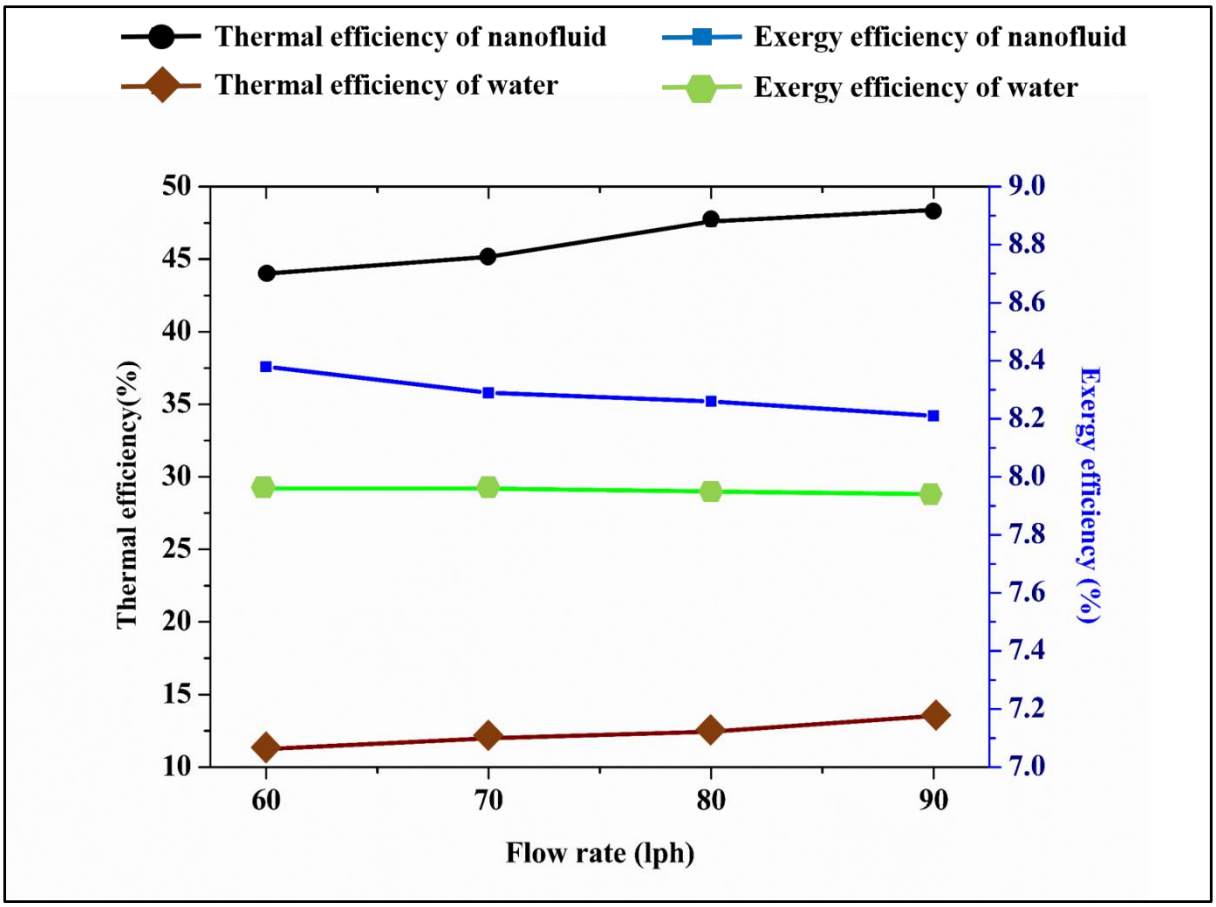

Fig. 12. Thermal efficiency and exergy efficiency at various flowrate.

Table. 5. Maximum temperature difference, thermal efficiency and exergy efficiency obtained for nanofluid and base fluid.

Flow rate (lph)	Temperature Difference (K)		Thermal Efficiency (%)		Exergy efficiency (%)	
	Base fluid	Nanofluid	Base fluid	Nanofluid	Base Fluid	Nanofluid
60	2.71	10.8	13.80	55.01	7.97	8.64
70	2.46	10.01	14.55	59.23	7.96	8.59
80	2.21	9.06	14.96	61.34	7.95	8.52
90	2.08	8.41	15.86	64.12	7.95	8.48

4. Conclusion

The study demonstrates the favourable influence of binary SiO_2/Ag-CuO nanofluid on augmenting the performance of volumetric absorption parabolic solar collector. The constituents in the nanofluid was optimised using the response surface methodology and desirability function. Nanofluid of optimum constituents (RTC of 1.234 and SRAF of

82.84%) was used as the working fluid in the volumetric absorption parabolic solar collector and the effect of flow rate on various performance parameters were estimated. The major findings are summarised as follows:

- A maximum temperature difference of 10.8K was observed for nanofluid at 60lph and 8.41K at 90 lph.
- SiO_2/Ag-CuO nanofluid improved the thermal performance of the collector with a maximum overall enhancement of 48.74% in thermal efficiency noted at a flow rate of 90lph.
- Increase in the flow rate leads to enhanced thermal efficiency of the collector, the maximum thermal efficiency of 55.01% and 64.12% were obtained at 60lph and 90lph.
- The presence of SiO_2/Ag-CuO nanofluid reduced the entropy generation and thus improved the exergy efficiency of the collector. However, entropy generation increased with the flow rate which in turn reduced the exergy efficiency.
- Exergy efficiency of collector using nanofluid was enhanced by 8.4% at 60 lph, in comparison with water.

REFERENCES

[1] Sanaz Akbarzadeh, Mohammad Sadegh Valipour, Heat transfer enhancement in parabolic trough collectors: A comprehensive review, Renew Sustain Energy Rev 92 (2018) 198–218 https://doi.org/10.1016/j.rser.2018.04.093

[2] R. Jain, R. Pitchumani, Fabrication and characterization of multiscale, fractal textured solar selective coatings, Sol. Energy Mater. Sol Cells 172 (2017) 213–219 https://doi.org/10.1016/j.solmat.2017.07.009

[3] G.C. Bakos, Ch. Tsechelidou Solar aided power generation of a 300 MW lignite fired power plant combined with line-focus parabolic trough collectors field, Renewable Energy 60 (2013) 540-547 https://doi.org/10.1016/j.renene.2013.05.024

[4] Jian-ping Meng, Xiao-peng Liu, Zhi-qiang Fu, Ke Zhang, Optical design of Cu/Zr0.2AlN0.8/ZrN/AlN/ZrN/AlN/Al34O62N4 solar selective absorbing coatings Sol. Energy 146 (2017) 430–435 https://doi.org/10.1016/j.solener.2017.03.012

[5] Xiaoxiao Yu, Yimin Xuan, Investigation on thermo-optical properties of CuO/Ag plasmonic nanofluids, Solar Energy 160 (2018) 200–207. https://doi.org/10.1016/j.solener.2017.12.007

[6] Tahereh B. Gorji, A.A. Ranjbar, A review on optical properties and application of nanofluids in direct absorption solar collectors (DASCs), Renew Sustain Energy Rev 72 (2017) 10–32 https://doi.org/10.1016/j.rser.2017.01.015

[7] Harriet Kimptona, Domenico Andrea Cristaldia, Eugen Stulzb, Xunli Zhang, Thermal performance and physicochemical stability of silver nanoprism based nanofluids for direct solar absorption, Sol. Energy 199 (2020) 366–376 https://doi.org/10.1016/j.solener.2020.02.039

[8] Shiva Gorjian, Hossein Ebadi , Francesco Calise , Ashish Shukla , Carlo Ingrao, A review on recent advancements in performance enhancement techniques for low-temperature solar collectors, Energy Convers. Manage 222 (2020) 113246 https://doi.org/10.1016/j.enconman.2020.113246

[9] Caiyan Qin, Joong Bae Kim, Bong Jae Lee, Performance analysis of a direct-absorption parabolic-trough solar collector using plasmonic nanofluids, Renewable Energy 143 (2019) 24-33 https://doi.org/10.1016/j.renene.2019.04.146

[10] Vishal Bhalla, Sachin Beejawat, Jay Doshi, Vikrant Khullar, Harjit Singh, Himanshu Tyagi, Silicone oil envelope for enhancing the performance of nanofluid based direct absorption solar collectors, Renewable Energy 145 (2020) 2733-2740 https://doi.org/10.1016/j.renene.2019.08.024

[11] Kongxiang Wang, Yan He, Pengyu Liu, Ankang Kan, Zhiheng Zheng, Lingling Wang, Huaqing Xie, Wei Yu, Highly-efficient nanofluid-based direct absorption solar collector enhanced by reverse-irradiation for medium temperature applications, Renewable Energy 159 (2020) 652-662 https://doi.org/10.1016/j.renene.2020.05.167

[12] Ahmet Z.Sahin, Mohammed Ayaz Uddin, Bekir S.Yilbas, AbdullahAl-Sharafi Performance enhancement of solar energy systems using nanofluids: An updated review, Renewable Energy 145 (2020) 1126-1148 https://doi.org/10.1016/j.renene.2019.06.108

[13] Sarkar J, Ghosh P, Adil A, A review on hybrid nanofluids: recent research, development and applications, Renew Sustain Energy Rev 43 (2015) 164–177 https://doi.org/10.1016/j.rser.2014.11.023

[14] Vishal Bhalla, Vikrant Khullar, Himanshu Tyagi, Experimental investigation of photo-thermal analysis of blended nanoparticles (Al_2O_3/Co_3O_4) for direct absorption solar thermal collector, Renewable Energy 123 (2018) 616-626 https://doi.org/10.1016/j.renene.2018.01.042

[15] Nan Chen, Haiyan Ma, Yang Li, Jinhu Cheng, Canying Zhang, Daxiong Wu, Haitao Zhu. Complementary optical absorption and enhanced solar thermal conversion of CuO-ATO nanofluids, Sol. Energy Mater. Sol Cells. 162 (2017) 83-92 https://doi.org/10.1016/j.solmat.2016.12.049

[16] Jia Zeng, Yimin Xuan, Enhanced solar thermal conversion and thermal conduction of MWCNT-SiO_2/Ag binary nanofluids, Appl. Energy, 212 (15) (2018), 809-819 https://doi.org/10.1016/j.apenergy.2017.12.083

[17] Pawel Keblinski, Jeffrey A. Eastman, David G. Cahill, Nanofluid for thermal transport, Mater. Today, 8 (6) (2005) 36-44 https://doi.org/10.1016/S1369-7021(05)70936-6

[18] Nor Azwadi Che Sidik, Muhammad Mahmud Jamil, Wan Mohd Arif Aziz Japar, Isa Muhammad Adamu, A review on preparation methods, stability and applications of hybrid nanofluids, Renew Sustain Energy Rev 80 (2017) 1112-1122 https://doi.org/10.1016/j.rser.2017.05.221

[19] Mikko Makela, Experimental design and response surface methodology in energy applications: A tutorial review, Energy Convers. Manage, 151 (2017) 630-640. https://doi.org/10.1016/j.enconman.2017.09.021

[20] Wenlian Ye, Peng Yang, Yingwen Liu, Multi-objective thermodynamic optimization of a free piston Stirling engine using response surface methodology, Energy Convers. Manage 176 (2018) 147–163
https://doi.org/10.1016/j.enconman.2018.09.011

[21] Sreehari Sreekumar, Albin Joseph, C.S. Sujith Kumar, Shijo Thomas, Investigation on influence of antimony tin oxide/silver nanofluid on direct absorption parabolic solar collector, J. Clean. Prod. 249 (2019) 119378
https://doi.org/10.1016/j.jclepro.2019.119378

[22] A. Kasaeian, S. Daviran, R. D. Azarian, A. Rashidi, 2015, Performance evaluation and nanofluid using capability study of a solar parabolic trough collector, J. Clean. Prod. 89 (2015) 368–375.
https://doi.org/10.1016/j.enconman.2014.09.056.

[23] E. Bellos, C. Tzivanidis, Thermal analysis of parabolic trough collector operating with mono and hybrid nanofluids, Sustain. Energy Technol. Assess. 26 (2018) 105-115.
https://doi.org/10.1016/j.seta.2017.10.005

[24] T.P. Otanicar, P.E. Phelan, J. S. Golden, Optical properties of liquids for direct absorption solar thermal energy systems, Sol. Energy 83 (2009) 969–977.
https://doi.org/ 10.1016/j.solener.2008.12.009.

[25] Yong Yang Gan, Hwai Chyuan Ong, Tau Chuan Ling, N.W.M. Zulkifli, Chin-Tsan Wang, Yung-Chin Yang, Thermal conductivity optimization and entropy generation analysis of titanium dioxide nanofluid in evacuated tube solar collector, Appl. Therm. Eng. 145 (2018) 155–164.
https://doi.org/10.1016/j.applthermaleng.2018.09.012

[26] Moffat, R.J., 1985. Describing the uncertainties in the experimental results. Exp. Therm. Fluid Sci. 1, 3-17.
https://doi.org/10.1016/0894-1777(88)90043-X.

[27] Salma Parvin, Rehena Nasrin, M.A. Alim, Heat transfer and entropy generation through nanofluid filled direct absorption solar collector, Int. J. Heat Mass Transfer 71 (2014) 386–395.
http://dx.doi.org/10.1016/j.ijheatmasstransfer.2013.12.043

[28] Albin Joseph, Sreehari Sreekumar, C S Sujith kumar, Shijo Thomas, Optimisation of thermo-optical properties of SiO_2/Ag-CuO nanofluid for direct absorption solar collectors, J. Mol. Liq. (2019) 111986.
https://doi.org/10.1016/j.molliq.2019.111986

[29] T. Aguilar, E. Sani, L. Mercatelli, I. Carrillo-Berdugo, E. Torres, J. Navas, Exfoliated graphene oxide-based nanofluids with enhanced thermal and optical properties for solar collectors in concentrating solar power, J. Mol. Liq 306 (2020) 112682.
https://doi.org/10.1016/j.molliq.2020.112862

[30] Omid Mahian, Ali Kianifar, Soteris A. Kalogirou, Ioan Pop, Somchai Wongwises, A review of the applications of nanofluids in solar energy, Int. J. Heat Mass Transfer 57 (2013) 582–594
http://dx.doi.org/10.1016/j.ijheatmasstransfer.2012.10.037

[31] M.M. Heyhat, M. Valizade, Sh. Abdolahzade, M. Maerefat, Thermal efficiency enhancement of direct absorption parabolic trough solar collector (DAPTSC) by using nanofluid and metal foam, Energy 192 (2020) 116662
https://doi.org/10.1016/j.energy.2019.116662

[32] M.A. Sharafeldin, Gyula Grof, Evacuated tube solar collector performance using

CeO2/water, nanofluid, J. Clean. Prod 185 (2018) 347-356
https://doi.org/10.1016/j.jclepro.2018.03.054

433

Energy and Exergy analysis of SiO_2/Ag-CuO plasmonic nanofluid on direct absorption parabolic solar collector

Albin Joseph[a], Sreehari Sreekumar[b], Shijo Thomas[a*]

[a] School of Materials Science and Engineering, National Institute of Technology, Calicut 673601, India

[b] Department of Mechanical Engineering, National Institute of Technology, Calicut 673601, India

Corresponding Author: Shijo Thomas, Email Address: shijo@nitc.ac.in

ABSTRACT

Experimental investigations on the application of SiO_2/Ag-CuO plasmonic nanofluid on direct/volumetric absorption parabolic solar collectors is presented in this article. The process variables for the preparation of nanofluid were optimised by employing the desirability function and response surface methodology (RSM). The optimisation was performed to achieve nanofluid with maximum possible thermal conductivity and solar absorptivity. The final solar radiation absorbed fraction and relative thermal conductivity noted for the optimised nanofluid was 82.84% and 1.234, respectively. The performance of the collector was evaluated at various flow rates from 60 lph to 90 lph, using water and optimised nanofluid as the heat transfer fluid. It is noted from the results that the thermal efficiency of the collector increases with the flow rate whereas, the exergy efficiency decreases for both water and nanofluid. The highest temperature difference of 11.27K was noted at 60lph for nanofluid which corresponds to a thermal efficiency of 57.47%. A maximum thermal efficiency of 64.05% was noted at 90 lph which corresponds to an enhancement of 48.19 % in comparison with water. Exergy efficiency of the nanofluid was enhanced by 9.4% at 60 lph, in comparison with water.

Keywords: Volumetric absorption parabolic solar collector, Binary nanofluid, Response surface methodology, Thermal efficiency, Entropy generation.

Nomenclature

.A	Area of parabola (m^2)	T_{in}	Inlet temperature (K)
A_p	Aperture width of parabola(m)	T_{sun}	Temperature of Sun (K)
C_p	Specific heat of working fluid (kJ/kg.K)	θ	Rim angle of the parabola
		σ	Uncertainty
E_{des}	Energy destruction (W)	τ_t	Transmittance of absorber tube
f	Focal length of the parabola (m)	r_r	Reflectivity of reflector
I	Solar irradiance (W/m^2)	η_{ex}	Exergy efficiency
m	mass flow rate (kg/sec)	η_{th}	Thermal efficiency
Q_u	Heat gained (W)	η_{opt}	Optical efficiency of the parabola
Q_s	Available direct solar energy (W)	RSM	Response surface methodology
Q_o	Energy loss (W)	RTC	Relative thermal conductivity
S_{gen}	Entropy generation (W/K)	SRAF	Solar radiation absorbed fraction
T_{amb}	Ambient temperature (K)	S1	Entropy generated during the transfer of heat to working fluid from solar irradiance
T_{out}	Outlet temperature (K)	S2	Entropy generated during the heat loss

1. Introduction

The persistent consumption of fossil fuels made them insufficient to meet the overwhelmingly increasing demand of energy. Stepping up the utilisation of sustainable energy sources is a widely acknowledged optimistic solution to meet the ever augmenting need for energy. Solar energy, a potential replacement to fossil fuels, provides high hope to overcome the energy crisis to a certain extent, especially in electricity generation and various heating application [1]. Solar energy being a sustainable and clean source of energy is gaining widespread attention for many thermal applications. A number of studies have been reported based on the solar energy conversions like solar thermal conversion, photo electric conversion and photo electric thermal conversion. The solar thermal convertors like dish collector, linear Fresnel reflectors (LFR) and parabolic trough collector (PTC) are the most preferred techniques for the medium and high temperature applications. In these techniques solar radiation is concentrated to a line or a point from which it is transferred to the working fluid (heat transfer fluid). Parabolic collectors are widely used for solar thermal application due to its better performance and comparative cost effectiveness. A parabolic trough collector is equipped with three components mainly, the parabolic reflector plate equipped with an absorber tube at its focal point and the working fluid inside the absorber tube. In a

typical operation of parabolic collector, solar ray is concentrated (using a parabolic reflector) towards the receiver tube placed at the focal line of the reflector, from which the converted energy in the form of heat is transferred by a working fluid for various applications like water heating, space heating, solar refrigeration system and even for power generation [2]. The solar thermal collectors could be coupled with various thermal systems like power generators, in order to improve the efficiency of the whole unit. Bakos and Tsechelidou [3] investigated solar trough collector coupled with the lignite fired steam power plant using a TRNSYS simulation software. They found that the Rankine efficiency of the plant improved from 33% to 37.64%. They also claim that the solar power plant could reduce the total fuel consumption and thus the CO_2 emission.

Apart from the design parameters of the parabolic collector, researchers now a days are focusing on the modification of absorber tubes. Solar absorptivity of the absorber tube is an important parameter that influences the performance of the collector [4, 23]. The absorber tube is an intermediate between the solar radiation and the working fluid. The absorption of solar energy will heat up the absorber tube. This heat is then conducted from the outer surface to the inner surface of the absorber tube which then is transferred to the heat transfer fluid/working fluid through convection. The intermediate heat losses through convection and radiation from the hot absorber tube surface to ambient, results in a deterioration in the performance of the collector [5, 22, 24]. This is where the concept of direct/volumetric absorption solar collectors gains significance by significantly reducing the thermal losses since the photo thermal conversion is directly achieved by the heat transfer fluid/working fluid [6]. Solar radiation absorption capability of the working fluid is the metric of performance of the volumetric absorption solar thermal conversion systems. The poor solar absorptivity of commonly used working fluids like deionised water, ethylene glycol, thermal oils, etc. renders them unfit for direct application in direct absorption collectors. Improving the solar absorptivity of these fluids is an area of active research [7, 8].

Nanofluids, with enhanced optical properties, are a suitable replacement for conventional heat transfer fluid in volumetric absorption solar collectors. Qin,et al. [9] made a performance evaluation of novel volumetric solar absorption parabolic collector using plasmonic nanofluids with constant absorption coefficient. An additional reflective coating was given on the upper half of the receiver tube that enhances the optical path length and investigations were performed by varying the receiver tube diameter. They concluded that thermal efficiency of the collector reduced with the diameter and at optimal diameter the direct absorption collector exhibit better performance than the conventional collectors. The

authors also claim that direct absorption parabolic collectors are effective at low flowrate ($\leq$0.18kg/s). As per the reports of Bhalla et al. [10] a layer of silicon envelope over the nanofluids could reduce the thermal losses due to convection to the atmosphere. The enhancement on temperature was nearly 3.5^{o}C. Wang et al. [11] introduced a novel technique which improved the efficiency of the direct absorption collector by introducing reverse irradiation. As per their observation the temperature within the fluid was almost uniform compared to the directed irradiated system, which establishes the influence of the nanoparticles in the fluid. However, the enhancement in the properties of nanofluid is limited up to a critical concentration, beyond which the properties of the nanofluid drops. The reason is attributed to reduced stability of the nanofluid at higher concentrations due to the agglomeration and sedimentation of the nanoparticles [28]. Recent reports [12] reveals that binary nanofluids exhibits better properties as compared to conventional nanofluids, due to the combined effect of two or more particles [13]. Bhalla at al. [14] investigated the influence of Al_2O_3/Co_3O_4 binary nanofluid on direct solar absorption system and compared it with that of the surface absorption system. The authors noticed 5.4^{o}C rise in the temperature for optimum direct absorption fluid compared to the surface absorption system. The reports of Chen et al. [15] reveals that improved optical properties are noted for binary nanofluid in which a broad absorption of solar radiation was observed. Zeng and Xuan [16] reports that the plasmonic effect of noble nanoparticles exhibits high photo thermal conversion. SiO_2/Ag is one of the commonly used plasmonic nanoparticles. However, the hybrid nanoparticles are found to be larger in size due to which the stability of the nanofluid is affected highly. As per the reports of Keblinski et al. [17] the particles size have very high impact on stability and properties of the nanofluid. The improved effectiveness of the nanofluid is observed at lower particle size. Thermo-optical properties of the nanofluid have very high significance in the direct absorption solar collector [29, 30]. Due to this reason it is highly recommended to employ working fluid with high thermal and optical properties in volumetric absorption solar collectors. From these perspectives, it is clear that the binary nanofluid in which more than one nanoparticles are dispersed, is capable to achieve both. The colloidal stability of the nanoparticles in the fluid is one of the main practical drawback associated with nanofluids. Nevertheless, this issue can be addressed by various methods like addition of surfactants, varying pH of the fluid, surface functionalization of the nanoparticles, etc. By enhancing the mutual repulsion between the particles, the chance of agglomeration of the particles and further sedimentation can be prevented. Zeta potential analysis is one of the method used to quantify the colloidal stability of nanofluids. An absolute value of zeta potential greater the

30 mv is considered to yield a stable nanofluid. However, for flow applications the issue of the stability is less pronounced since the fluid under circulation is in continuous agitation [18].

In the present study the performance evaluation of the volumetric absorption collector using plasmonic SiO_2/Ag-CuO binary nanofluid is investigated experimentally. Additional advantages on photo-thermal conversion of nanofluid could be observed in SiO_2/Ag particles due to the plasmonic effect, the thermal transport within the nanofluid is being influenced by the CuO nanoparticles. The desirability function combined with the response surface methodology (RSM), a widely adopted technique in industries for multi objective response process, was used to optimise the process variables involved in the study [19, 20]. The experiments were conducted at National Institute of Technology Calicut (latitude: 11.3216, longitude: 75.9336). Thermo-optical properties exhibited by the nanofluid as well as the collector efficiency and entropy generation of the collector are analysed using the optimised SiO_2/Ag-CuO nanofluid, and compared with base fluid. Even though many lab scale studies on the optical properties of plasmonic nanofluid were reported, to the best of the author's knowledge this is the first attempt that investigates the influence of a plasmonic binary nanofluid on a volumetric absorption parabolic collector.

2. Materials and methods

2.1 Synthesis of SiO_2/Ag-CuO nanofluid.

SiO_2/Ag-CuO nanofluid was synthesised by two step method in which the particles are added and dispersed in the water. SiO_2/Ag particle used in the fluid was prepared by introducing Ag on the SiO_2 by reducing $AgNO_3$ with $SnCl_2$. CuO nanoparticles used are directly purchased from Sigma Aldrich. To achieve a stable suspension, sodium dodecyl sulfonate was used as surfactant. Optimisation of the concentration of nanoparticle and surfactant were done using a desirability function. The detailed procedure of synthesis of nanofluid and optimisation is mentioned in the earlier investigation conducted by the same authors [28]. The optimised nanofluid is then used in the volumetric absorption solar collector.

2.2. Design and manufacturing of experimental setup.

2.2.1 Parabolic reflector

The length of parabolic trough is 1500 mm and the aperture width is 1080 mm. Three troughs of dimensions 500 mm length and 1080mm aperture diameter each were fabricated using the glass wool - epoxy composite. Anodised aluminium sheets were used as the reflector. The reflector sheets were fixed on the glass wool-epoxy composite parabolic trough so that the reflector attain the parabolic trough shape. The rim angle of the parabola is 90^o and Eq. 1 represents the parabolic profile of the fabricated trough.

$$Y = 0.925X^2 \quad (1)$$

The focal point of the parabola is given by equation 2

$$f = \frac{Ap}{2} Cot\theta + \frac{Ap^2}{16\, f} \quad (2)$$

Where f is focal length of the parabola, θ is the rim angle and A_p, the aperture width of the parabola.

The dimensions of the parabolic trough are presented in Table 1.

Table. 1: Dimension of parabolic trough fabricated.

Parameter	**Dimension**
Length of parabola	1.5 m
Distance of focal point	0.272 m
Aperture width	1.05m
Aperture Area	1.575 m^2
Rim angle	90^o
Outer tube inner diameter	0.035 m
Inner tube inner diameter	0.015 m

2.2.2 Absorber Tube.

Optical absorptivity and other dimensions of the absorber tube highly influences the thermal and optical efficiency of a parabolic solar collector. In the present system, glass-glass absorber tube made of quartz is used, which enable high transmittance, reducing the optical losses of absorber tube. Moreover, the evacuation of glass- glass annulus could reduce the convective heat losses [10]. A provision was made on the experimental setup to adjust the position of the absorber tube so as to maintain the absorber tube exactly at the focal point of

the parabolic trough. Both ends of the absorber tube were sealed using Teflon coupling which could withstand temperature up to 350^{o}C and high temperature RTV silicon (anabond) was used as sealant.

2.2.3 Solar Tracker

Continuous tracking of sun is mandatory for the collector to get perpendicular rays on its surface. To accomplish this a solar tracker was employed. The tracker consist of a geared motor which is connected to the axis of parabolic collector. The sun tracking was achieved using an LDR photo resister as the sensor. The LDR sensor unit (not clear in the figure due to its small size) placed on the trough is connected to geared motor unit with an intermediate PCB circuit.

2.2.4 Experimental procedure.

The parabolic trough collector used in the present study is located at National Institute of Technology, Calicut in the North-South direction (latitude: 11.3216, longitude: 75.9336). The experiment was carried out on clear sunny days during the month of March and April. The hydraulic cycle chosen for the study is shown in Fig 1. According to Fig 1 the nanofluid from a reservoir is pumped to the parabolic collector and then to a heat exchanging unit (constant temperature bath). The heat exchanger cools the nanofluid and maintain a constant temperature at the inlet of absorber tube. The nanofluid from the heat exchanger is finally directed to the reservoir. The flow rate of the nanofluid was varied using a valve and flow meter. The inlet and outlet temperatures were noted using calibrated T-type thermocouples, connected to a data logger (Agilent). The temperatures were noted at every 5 minutes interval from 09:45 am to 4:15 pm and average temperature for every 30 minutes were determined.

As mentioned in Section 2.2 the nanofluid was synthesised based on the range of concentration mentioned in Table 3 and its thermo-optical properties were measured. An optimised process variables of nanofluids were achieved that enables maximum possible solar radiation absorption and thermal conductivity. The nanofluid prepared using this optimised combination is further experimentally analysed to quantify its effect on volumetric absorption parabolic collector (VAPC). The influence of this nanofluid on VAPC at various flow rates starting from 60 lph to 90 lph, were analysed and compared with that of base fluid.

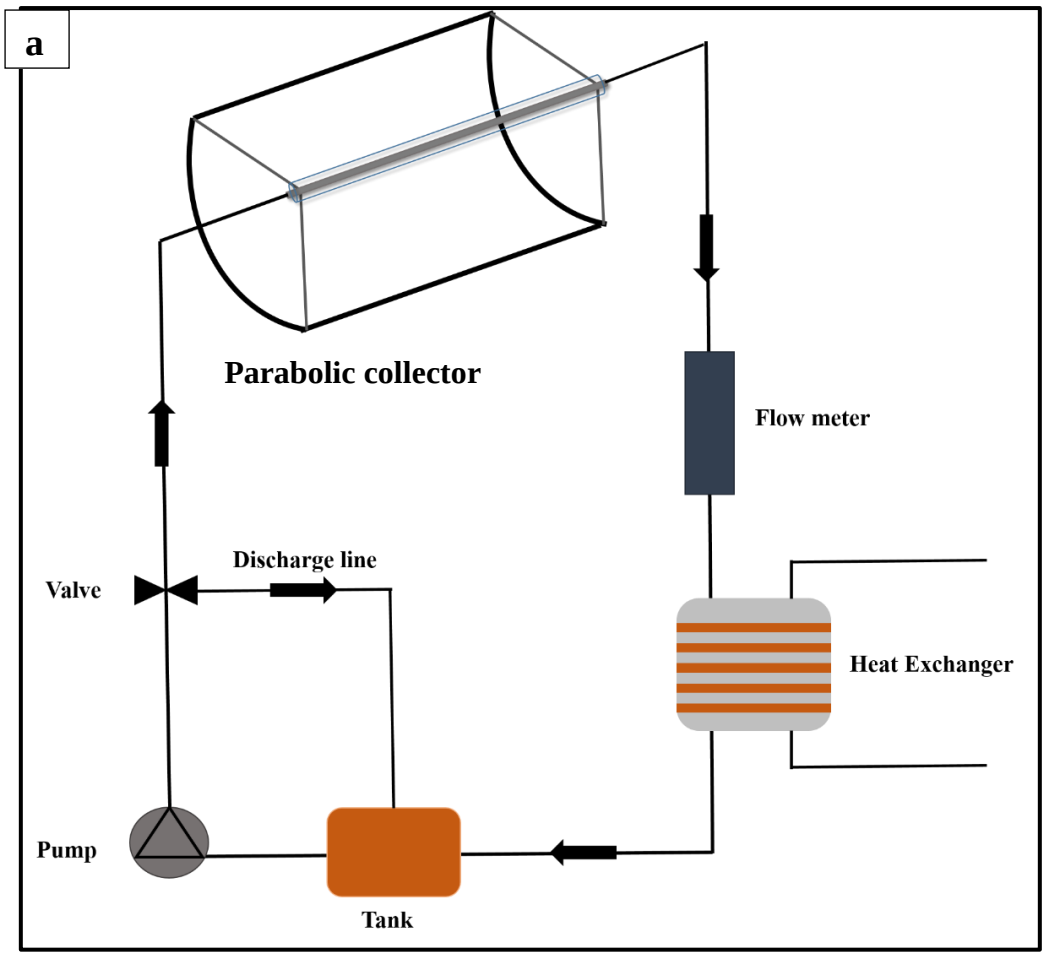

197

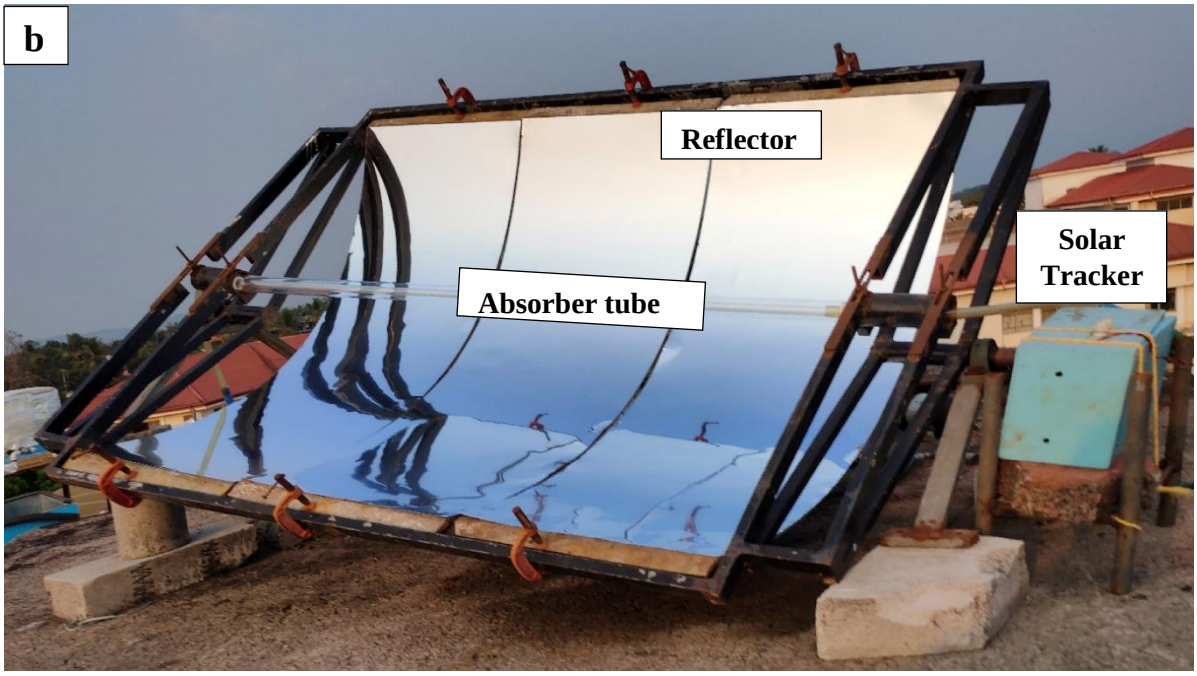

198

199 Fig. 1. a) Schematic of experimental setup, b) Photograph of fabricated parabolic trough

200

2.3 Mathematical formulation

Mathematical formulation used for the estimation of performance parameters are listed below:

Useful heat produced (W):

$$Q_u = m.Cp.(T_{out} - T_{in}) \quad (3)$$

Available direct solar energy:

$$Q_s = A.I \quad (4)$$

Optical and thermal efficiency of the parabola was calculated using equation 5 and 6

$$\eta_{opt} = \tau_t r_r \quad (5)$$

$$\eta_{th} = \frac{Q_u}{Q_s} \quad (6)$$

Entropy generation (W/K):

$$S_{gen} = mCp\ ln(\frac{T_{out}}{T_{in}}) - \frac{Q_s}{T_{Sun}} + \frac{Q_o}{T_{amb}} \quad (7)$$

The entropy generation during the heat transfer from sun to nanofluid and inside absorber tube was estimated using Eq 7. The entropy generated due to the pressure drop during fluid flow is neglected as it was insignificant.

$$Q_o = Q_s - mC_p\ (T_{out} - T_{in}) \quad (8)$$

Energy destruction (W):

$$E_{des} = S_{gen} \times T_{amb} \quad (9)$$

Exergy efficiency:

$$\eta_{Ex} = 1 - \frac{T_{amb} \times S_{gen}}{\left[1 - \frac{T_{amb}}{T_{sun}}\right] Q_s} \quad (10)$$

2.4 Experimental Uncertainty Analysis

The uncertainty experimental data was estimated using the method descried by Moffat [26]. Table 2 presents the estimated uncertainty of various parameters. The calibration of thermocouple was done by employing a constant temperature bath as standard. The maximum error in the thermocouple was found to be ± 0.1K, the uncertainty of Heat gained, thermal and exergy efficiency was calculated from the equation 11-13

$$\frac{\sigma Qu}{Qu} = \sqrt{\left(\frac{\sigma m}{m}\right)^2 + \left(\frac{\sigma T_{in}}{T_{in}}\right)^2 + \left(\frac{\sigma T_{out}}{T_{out}}\right)^2} \quad (11)$$

$$\frac{\sigma \eta_{th}}{\eta_{th}} = \sqrt{\left(\frac{\sigma m}{m}\right)^2 + \left(\frac{\sigma T_{in}}{T_{in}}\right)^2 + \left(\frac{\sigma T_{out}}{T_{out}}\right)^2 + \left(\frac{\sigma I}{I}\right)^2} \quad (12)$$

$$\frac{\sigma \eta_{Ex}}{\eta_{Ex}} = \sqrt{\left(\frac{\sigma m}{m}\right)^2 + \left(\frac{\sigma T_{in}}{T_{in}}\right)^2 + \left(\frac{\sigma T_{out}}{T_{out}}\right)^2 + \left(\frac{\sigma T_{amb}}{T_{amb}}\right)^2 + \left(\frac{\sigma I}{I}\right)^2} \quad (13)$$

Table. 2: Uncertainties of variables

Variables	Uncertainty
Flow rate	≤± 2.5 %
Solar irradiance	≤ ± 5.00 W/m^2
Heat Gained	≤ ± 2.53 %
Thermal efficiency	≤ ± 2.6 %
Exergy efficiency	≤ ± 2.62 %

3. Result and discussion

3.1 Characterisation of nanofluids

Characterisation was limited to measurement of solar absorptivity and thermal conductivity of nanofluid and morphological analysis of nanoparticles. Data obtained from the UV-vis spectrometer (Avantes) was used to estimate the solar radiation absorbed fraction (SRAF). To quantify the thermal conductivity exhibited by the nanofluids, a thermal properties analyser (KD2 pro) was employed. Morphology of the nanoparticles were analysed using the field emission scanning electron microscope (Hitachi SU 6600) and are presented in Fig 2.

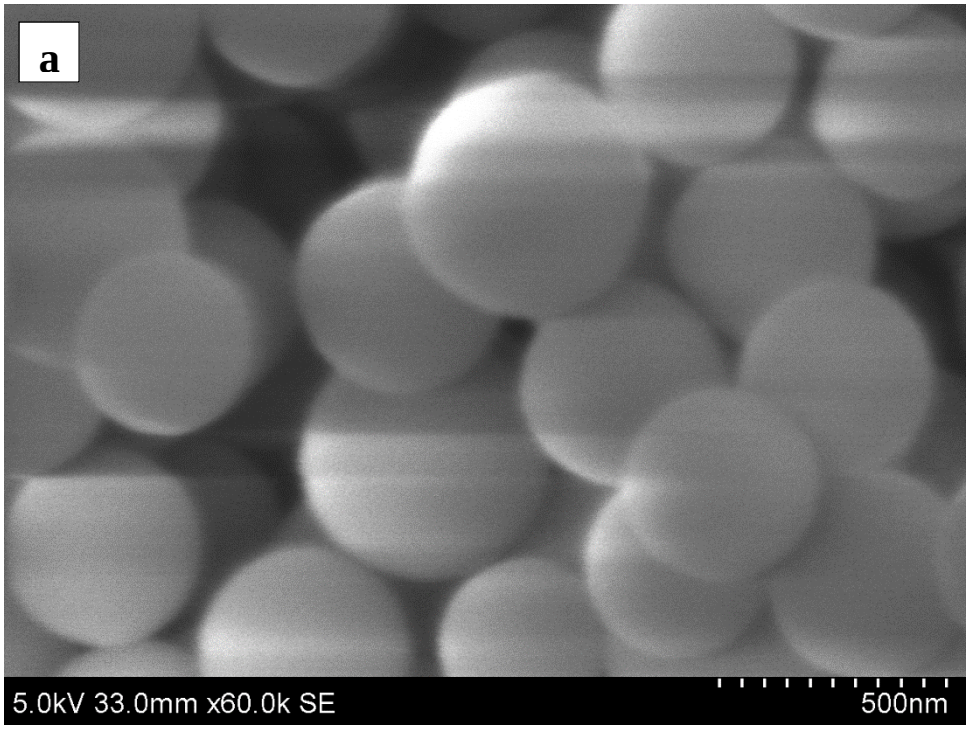

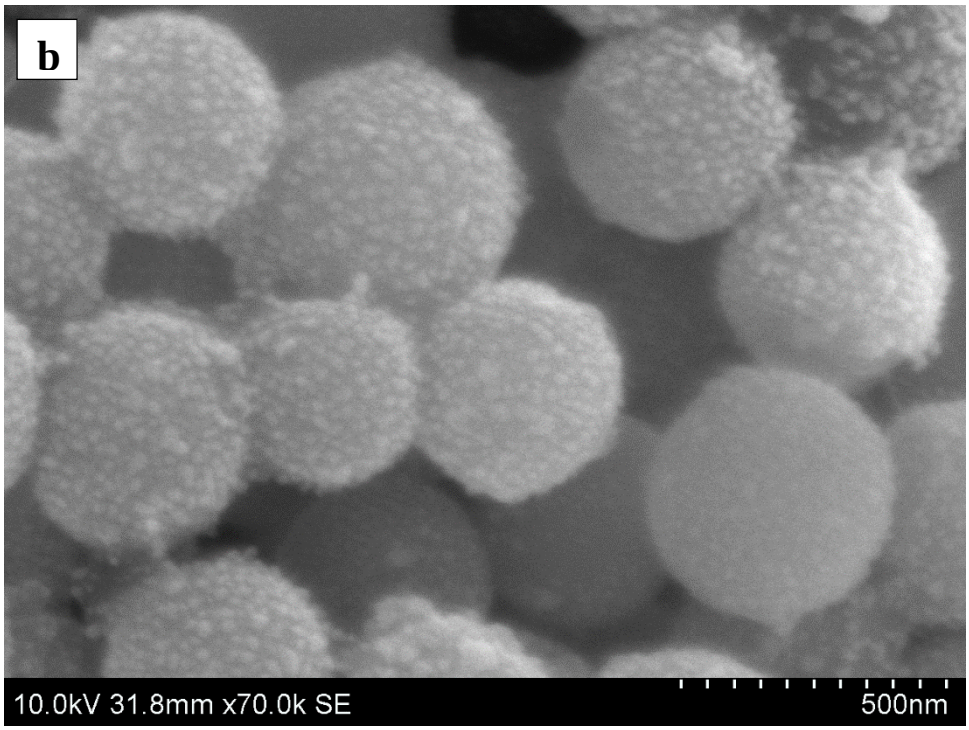

Fig. 2. SEM images a) SiO_2, b) SiO_2/Ag nanoparticles.

3.2 Optimisation of SiO_2/Ag-CuO plasmonic binary nanofluid

The optimisation of the nanofluid is detailed in the earlier publication by the same authors [28]. Desirability approach on RSM was adopted to optimise the process variables involved in the synthesis of nanofluid. Desirability function is a widely adopted approaches

to optimise multi objective problems [20]. The regression equation for relative thermal conductivity and SRAF obtained from the central composite design of response surface methodology (Eq. 14 and 15) was taken for the desirability approach [28]. The objective of the optimisation was to maximise SRAF and thermal conductivity of the nanofluids. In this approach the variables such as mass of nanoparticles like SiO_2/Ag and CuO, surfactant are in the design range (between upper limit and lower limit), while the responses like thermal conductivity and SRAF are set to be maximal. Table 3 presents the goal, lower and upper limit and importance of each process variables. The optimal combination of process variables was obtained as 206.3 mg of SiO_2/Ag per litre of DI water and correspondingly, 864.7 and 1996.2 mg of CuO and SDS respectively. Figure 3 shows the variation of desirability with change in concentration of particles. It can be seen that, the desirability drops after concentration of SiO_2/Ag particles exceeds 206.3 mg/l, which might be due to the fact that beyond this concentration the stability of the nanofluid decreases resulting in a decrease in thermal conductivity and SRAF. However, the desirability increased with the concentration of CuO and then drops after 864.7mg/l. This could be due to the fact that, as the CuO concentration increases the thermo-optical properties are found to be increased and after a critical concentration the stability of the nanofluid was affected, thus decreasing the desirability. Moreover, the stability was found to be increased with surfactant concentration due to which the desirability increases with the concentration of surfactant. The optimised concentrations of nanoparticles were found to be stable with a zeta potential of -38.7mV. The RTC and SRAF for the optimised concentration were found to be 1.234 and 82.84% respectively from the response equations. To confirm this experimentally, the optimised nanofluid combination was prepared and the experimental value of RTC and SRAF were obtained as 1.231 and 81.79% respectively. Since the predicted and experimental values are comparable to each other in addition with the desirability value of one, the results are reliable. The final optimised nanofluid is then taken to the parabolic collector for the analysis of photo thermal conversion and entropy generation. In addition thermal conductivity of the optimised nanofluid in the temperature range, 30^{o}C to 50^{o}C, was measured and presented in the Table 4. The relative thermal conductivity (Thermal conductivity of nanofluid by thermal conductivity of water) was also estimated.

.

$$RTC = 1.11825 + (4.64016\times10^{-005} \times C) + (8.23773\times10^{-006} \times B) - (7.08371\times10^{-005} \times A) - (2.81400\times10^{-008} \times A \times B) + (7.00727\times10^{-008} \times B \times C) - (1.48865\times10^{-008} \times A \times C) -$$

283 $(1.87837x10^{-008} \times C^2) - (6.43326x10^{-009} \times B^2) + (3.11178x10^{-008} \times A^2)$

284 (14)

285 SRAF = 35.2379 + (0.039759 x C) + (0.010745 x B) + (0.021866 x A) - (3.34793E-006 x A

286 x B) – (6.48624 $x10^{-006}$ x B x C) - (6.67764 $x10^{-006}$ x A x C) - (7.30303 $x10^{-006}$ x C^2) -

287 (1.95099 $x10^{-006}$ x B^2) - (1.08898 $x10^{-005}$ x A^2)

288 (15)

289 Where A, B, and C are mass of SiO_2/Ag, CuO and SDS respectively per litre of DI water.

290

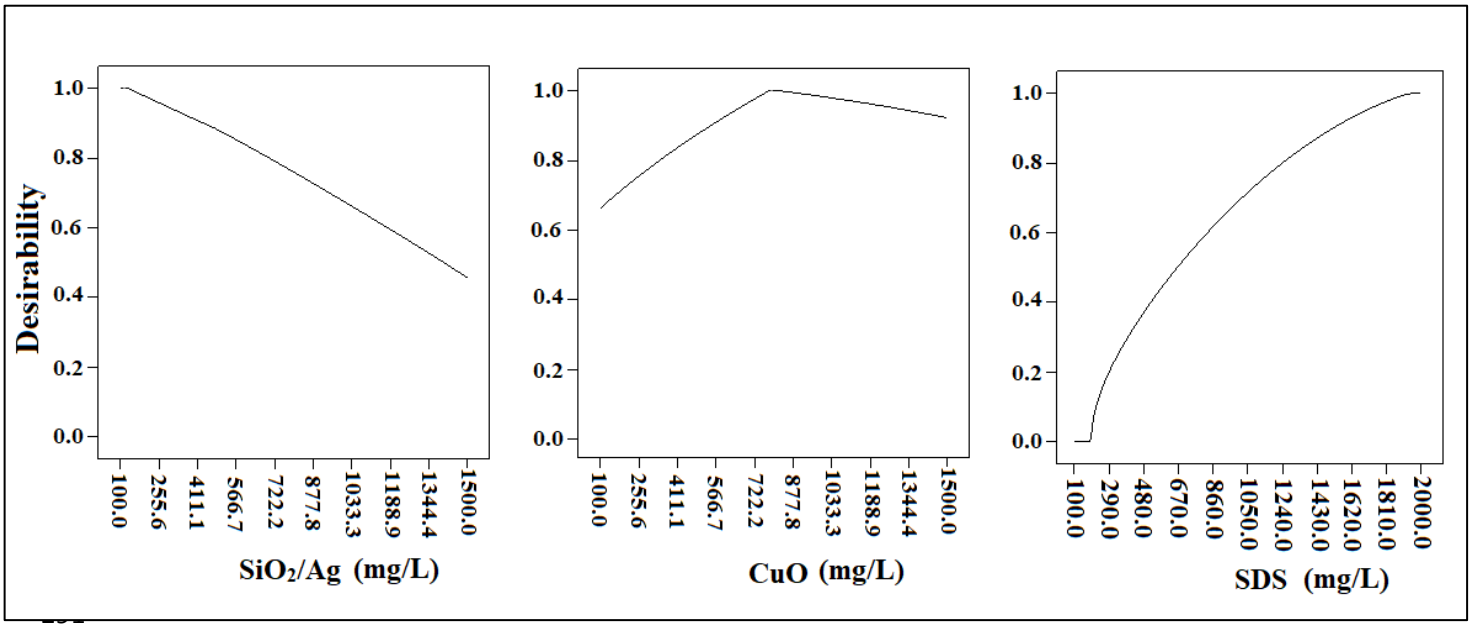

292 **Fig .3.** Variation of desirability function with process variables.

293 **Table. 3:** Conditions adopted during the optimisation.

Name	Goal	Lower limit	Upper limit	Importance
Concentration of SiO_2/Ag (mg/l)	In range	100	1500	4
Concentration of CuO (mg/l)	In range	100	1500	4
Concentration of SDS (mg/l)	In range	100	2000	4

294

295

Table 4. Thermal conductivity at various temperature

Temperature (^oC)	Relative thermal conductivity	Thermal conductivity (W/mK)
30	1.234	0.7404
35	1.248	0.7491
40	1.262	0.7576
45	1.299	0.7794
50	1.314	0.7886

3.3 Performance of SiO_2/Ag-CuO hybrid plasmonic nanofluid on parabolic collector.

The SiO_2/Ag-CuO nanofluid used as working fluid in the parabolic collector was prepared based on the optimum process variables achieved from the procedure mentioned in 3.2. The optimised valued of mass of particles and surfactant (process variables for preparing the nanofluid) are 206.3 mg/L, 864.7mg/L and 1996.2mg/L of SiO_2/Ag, CuO and SDS respectively. The experiment was carried out on a sunny day during the month of March and April. The Average solar radiation in the experimental location was 850 W/m^2. The maximum radiation noted was 950W/m^2 which mostly occur during 12:00 pm to 2:00 pm.

Figure 4 presents the temperature profile of nanofluid and the base fluid at various flow rates. The temperatures were noted from 10:00 am to 4:00 pm. As the figure says the temperature difference decreases with the increase in flow rate of working fluid. A maximum temperature difference of 11.27K was noted for the optimum nanofluid at the flow rate of 60 lph and 8.4K at 90 lph. The highest noted temperature difference for water was 2.61K, at 60lph. Table 4 shows the maximum temperature difference obtained for SiO_2/Ag-CuO nanofluid and water at various flow rates. It is apparent that the introduction of nanoparticles enhanced the performance of the collector by improving the optical and thermal properties of the nanofluid. The improved solar absorptivity of the nanofluid increased the solar thermal conversion of the collector and the enhancement in thermal conductivity augmented the heat transfer for nanofluids. The experiments were repeated three times and the reported values are the average, to ensure the repeatability. The variation of temperature difference with solar radiation is plotted and added in the manuscript as Figure 5. As can be seen form the figure the temperature difference increases with the solar radiation for a particular flow rate and the variation is almost linear. At a flow rate of 60 lph, the maximum temperature difference obtained was 10.8 ^oC for 930 W/m^2. The minimum temperature difference observed at this flow rate was 5.16 ^oC at a solar radiation of 720 W/m^2. The maximum temperature noted at 90 lph was 8.41 ^oC at 930 W/m^2 for which the maximum efficiency was also obtained. The

maximum observed temperatures were 10.21 ^{o}C and 8.96 ^{o}C at flow rates of 70 and 80 lph respectively for a solar radiation of 930 W/m^2

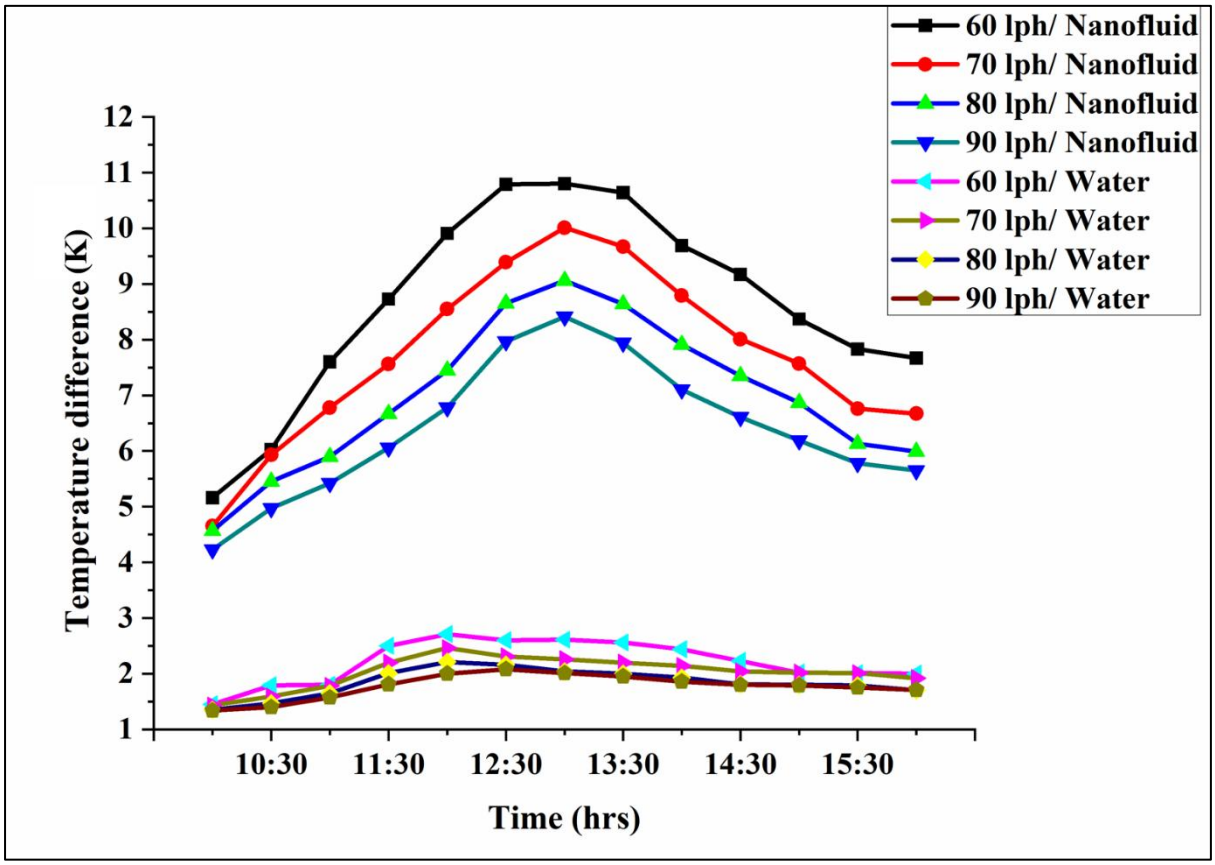

Fig. 4. Temperature profile of nanofluid and water at various flow rates.

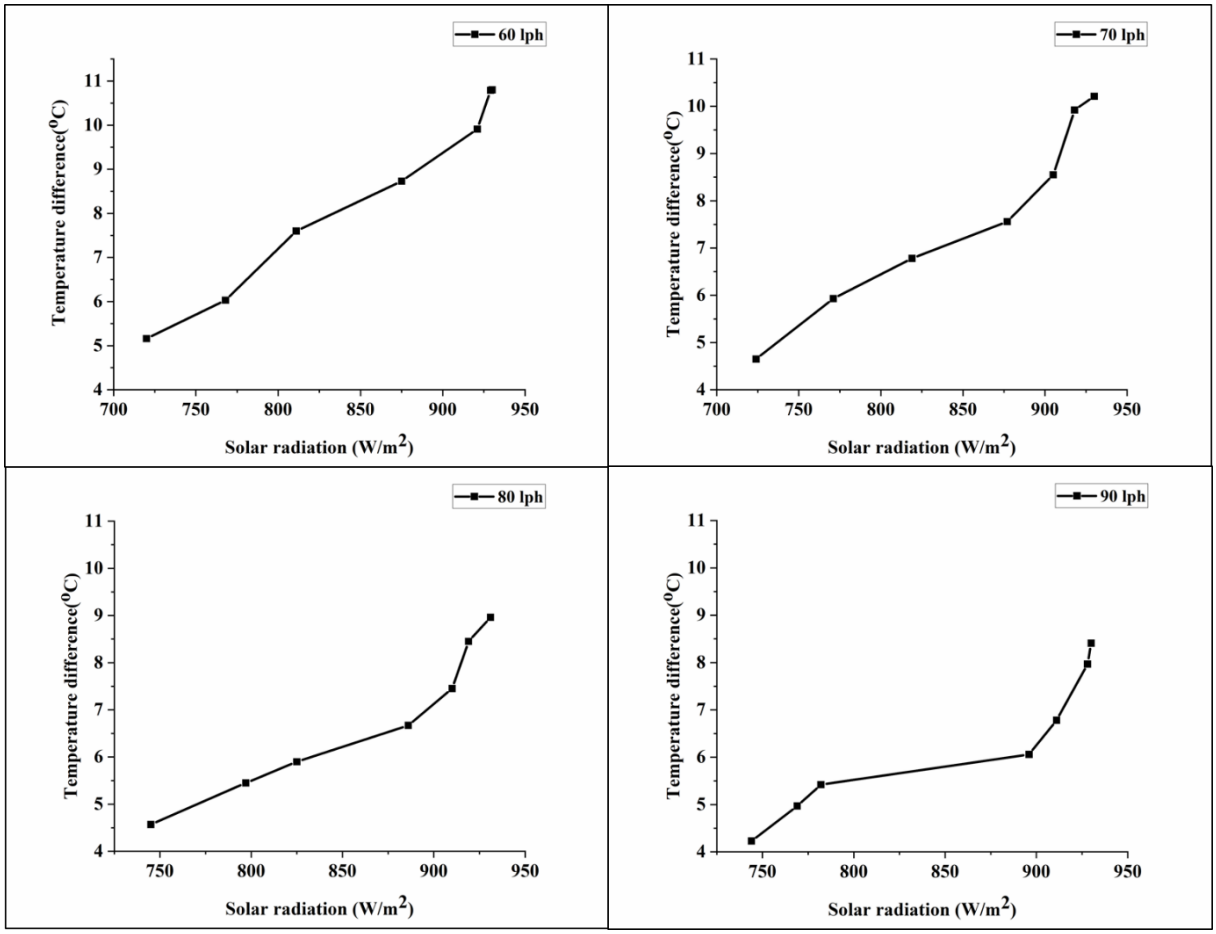

328

329 **Fig. 5** Variation of temperature difference with radiation.

330

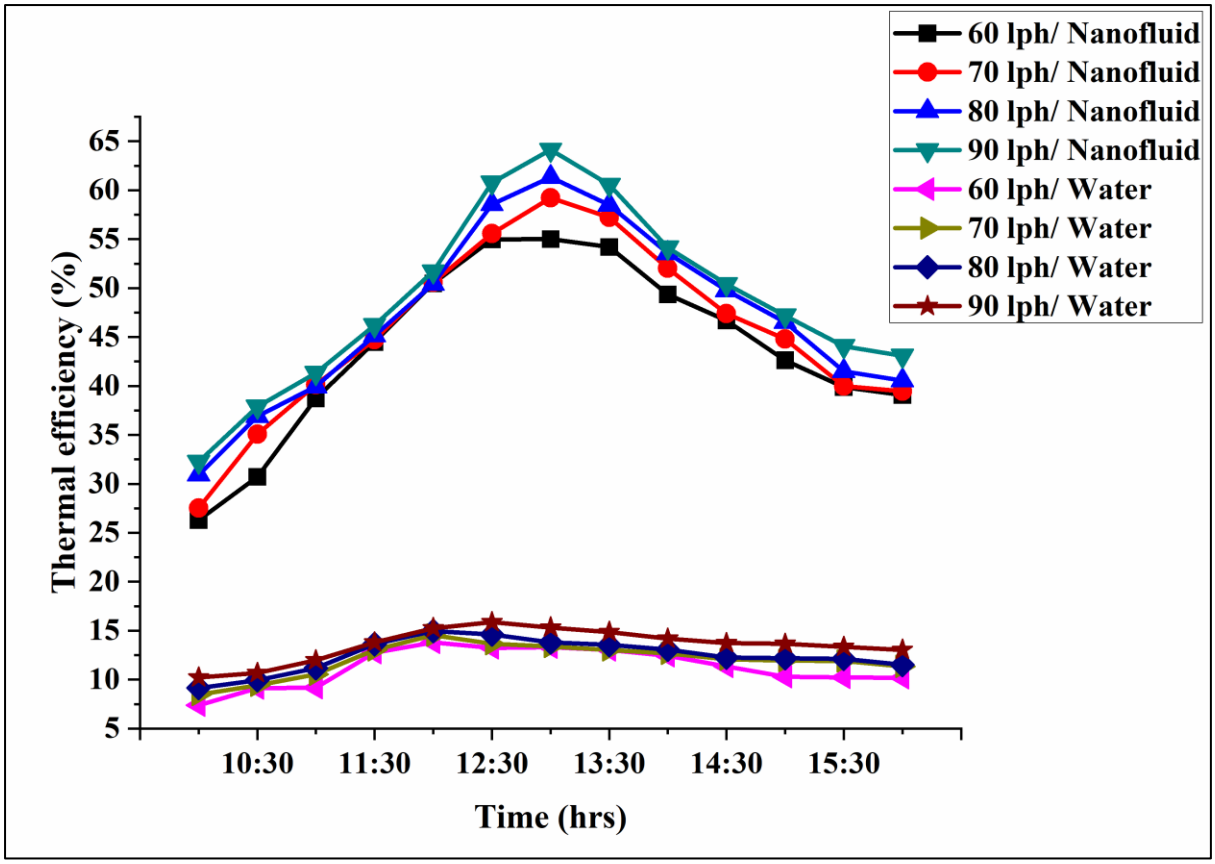

Fig. 6. Thermal efficiency plot of nanofluid and water at various flow rates.

The thermal efficiency of the collector was estimated using the equations 3, 4, 5 and 6. The transient variation of collector efficiency at various flow rate are shown in Fig. 6. The direct solar irradiance is 850 W/m^2, which is the estimated average solar radiation at the location. The maximum thermal efficiencies for water are 13.29, 14.55, 14.96 and 15.86% at flow rates of 60, 70, 80 and 90 lph, respectively. The corresponding values of efficiencies estimated for nanofluid are 57.40, 60.41, 63.72 and 64.13% respectively. In addition, it could be observed from Fig. 6 that the maximum efficiency was obtained during the time period of 12:00 pm to 2:00 pm. As mentioned before, the efficiency of the collector depends on the thermo-optical properties of the working fluid. Plasmonic SiO_2/Ag nanoparticles used in the present investigation exhibited an additional improvement in the optical absorptivity of the fluid which in turn resulted in better photo thermal conversion. It is reported that in comparison with other nanoparticles plasmonic nanoparticles exhibit an additional self-heating due to the plasmonic effect, which in turn enhance the photo thermal conversion efficiency of the nanofluid [16, 21]. The presence of CuO in the fluid transfers the absorbed

348 solar energy effectively, which is attributed to its higher thermal conductivity [17]. Reynolds
349 number is another parameter that influences the efficiency of the collector. The heat transfer
350 becomes more effective as the Reynolds number/ flow rate increases which also results in the
351 increased efficiency of the collector [25, 31]. As explained in equation (6) thermal efficiency
352 of the collector is defined as the ratio of useful heat produced to the available direct solar
353 energy. As the flow rate increases the amount of useful heat carried away by the working
354 fluid increases. As the flowrate increases the local mixing between the fluid and solid
355 particles and also between the fluid and the tube surface increases which results in enhanced
356 thermal transport and reduced thermal loss [32].

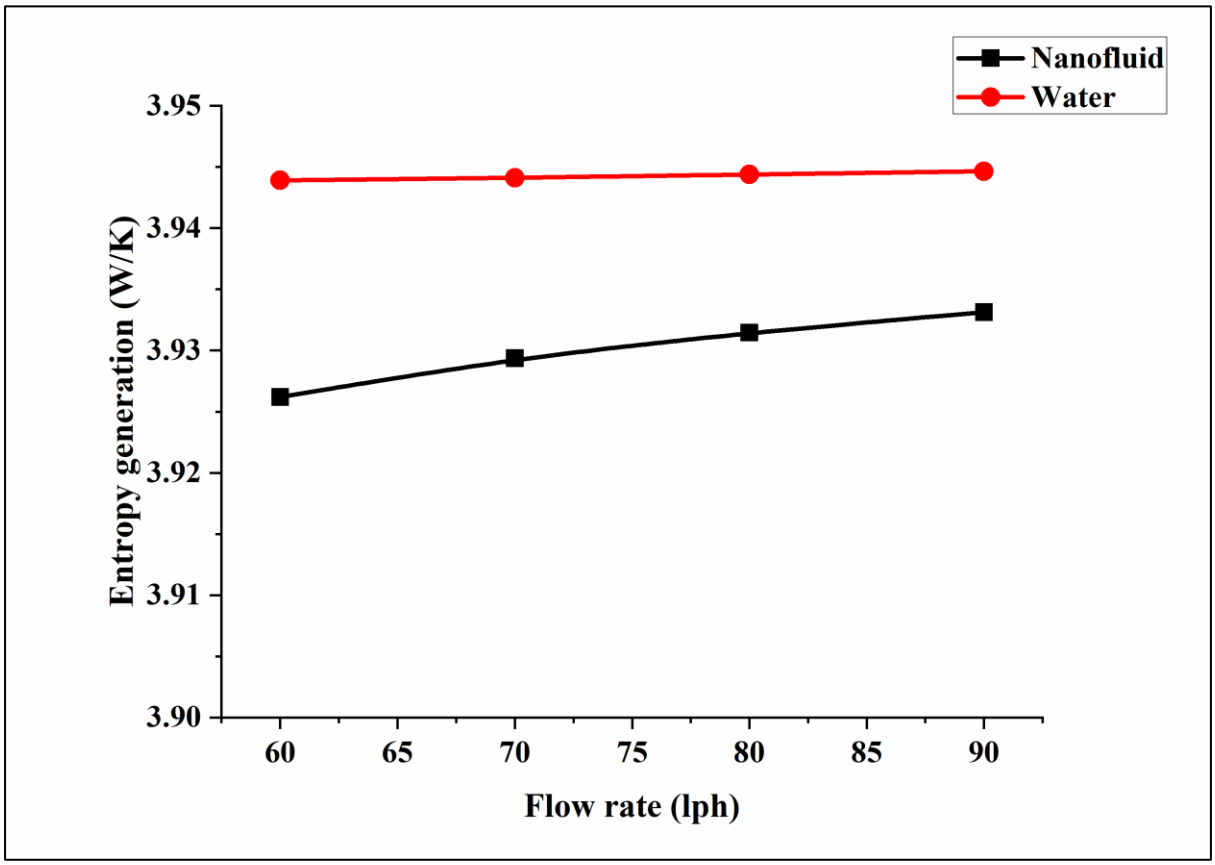

357

358 **Fig. 7.** Average entropy generation at various flowrates.

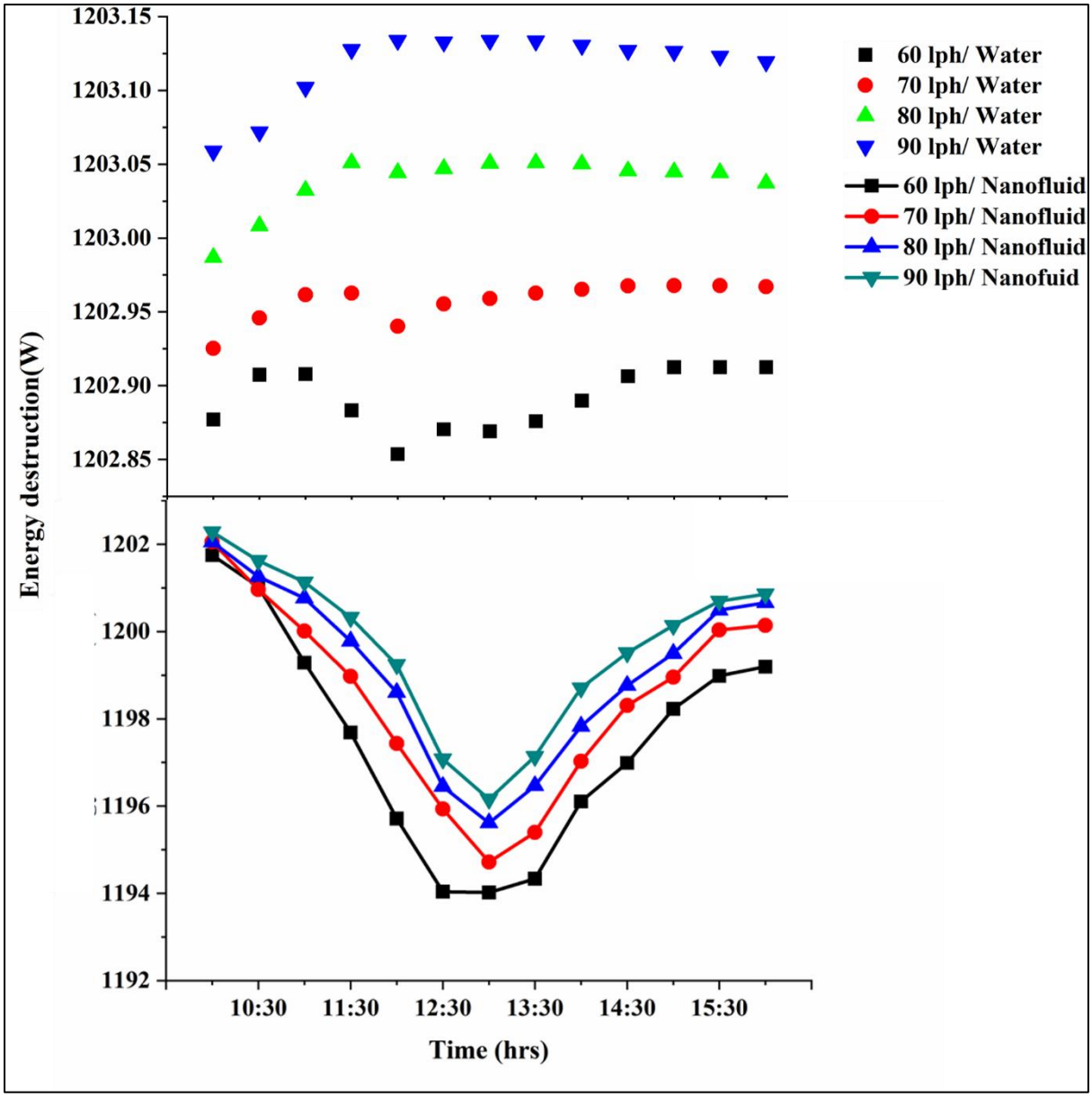

Fig. 8. Energy destruction profile of nanofluid and water at various flowrates.

Figures 7 and 8 shows the entropy generation and energy destruction calculated using equations 7, 8, 9 and 10. As can be seen from Figure 7, the entropy generation slightly decreased with the dispersion of nanoparticles in water. The entropy generation was almost constant with change in flow rate in the case of water, while it slightly increased with flowrate for nanofluid. In the present study, two factors could be accounted for the entropy generation. 1) Entropy generation due to the heat transfer from solar irradiance to the nanofluid (S1). 2) Entropy generated during to the heat loss from the nanofluid to the surroundings (S2). The contribution of the two sources (S1 & S2) to entropy generation in water and nanofluids at different flow rates is shown in Fig. 9. Among these two sources, the

entropy generation due to the heating up of the nanofluid as it flows through the collector tube from inlet to outlet (S1) was found to be lesser than the entropy generation due the heat losses from the nanofluid (S2). At a flowrate of 90 lph the S1 for water was 72.14% lower than that of nanofluid. The S1 for water was found to be less compared to nanofluid since the heat gain was less in water when compared to nanofluid. However, entropy generated due to the losses (S2) was found to be less compared to water and reduces with the flow rate for nanofluids. At a flowrate of 90 lph the S2 for water is 81.54% higher than that of nanofluid. The contribution of entropy generation due to heat losses (S2) of water being much higher than that of nanofluid is the reason for the slight increase in overall entropy generation (S1+S2) of water with flow rate. On comparing figures 10 and 11 with Fig. 4 it can be seen that, at a particular flow rate S1 increases with temperature difference whereas S2 decreases (Fig 10 and 11). The higher absorption of heat by the plasmonic nanofluids results in higher temperature gain of the fluid and thus contributes to S1. In spite of the high temperature rise of the fluid the heat losses to the ambient is lesser in volumetric absorption systems employing plasmonic nanofluids is evident from the decreasing S2 values. The variation of thermal efficiency and exergy efficiency with the flow rate is presented in Fig 12. It can be seen that in the case of the optimised nanofluid, the exergy efficiency shows a slight decrease with flow rate, while thermal efficiency increases. But the exergy efficiency of the nanofluid was found to be higher than that of water with an enhancement of 9.4% at 60 lph. It could be surmised that the energy losses associated with the volumetric absorption system reduces with the flow rate while employing nanofluid, while the generated entropy during the gain of heat from the sun increases with the flow rate. The increase in overall generation of entropy is attributed to the development of temperature drop between the top wall of the collector and the outlet due to the enhanced heat gain [27]. In addition, unlike the surface absorption based parabolic collector, in volumetric absorption solar collector the working fluid directly absorbs and convert the solar irradiance. Since the absorbing medium is in a kinematic state, the flow rate directly affects the conversion of solar energy to heat. At higher flow rate of working fluid, the energy conversion might be incomplete due to the insufficient time available for the energy absorption owing to the rapid motion of nanoparticles in the working fluid.

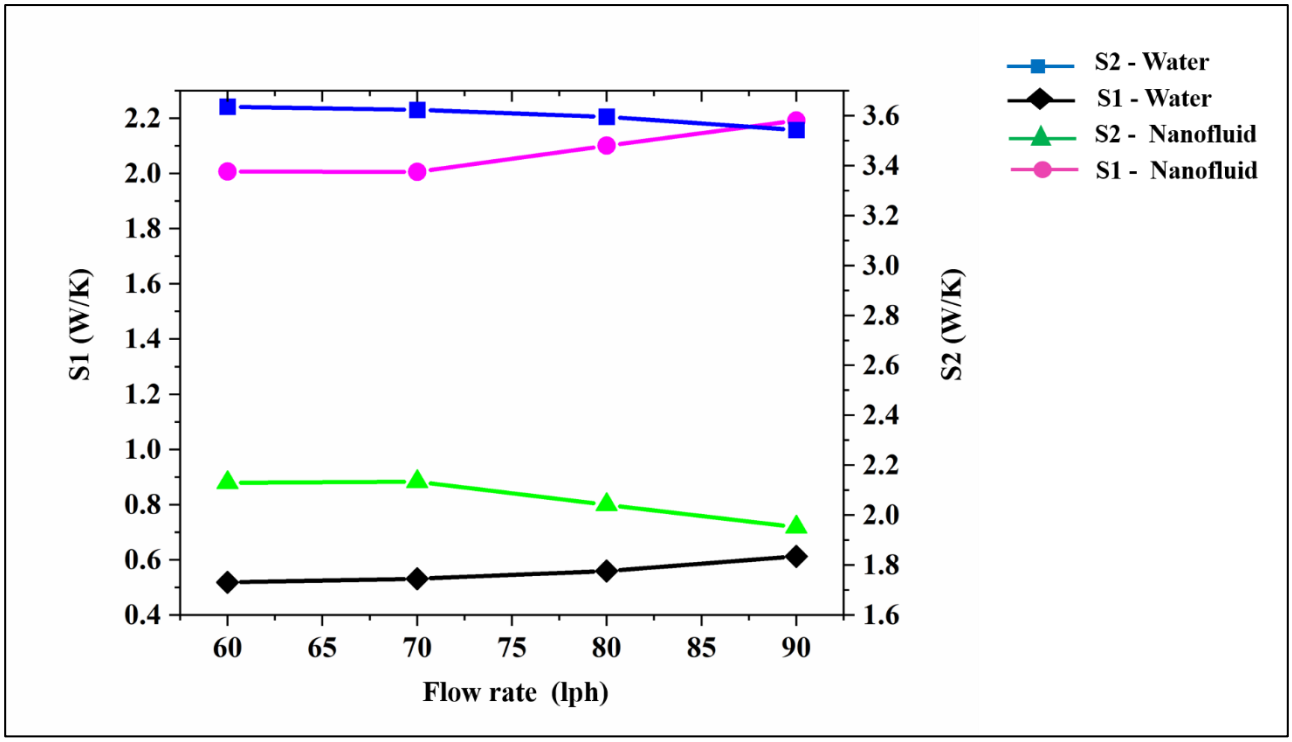

399

400 **Fig. 9**. Variation of average S1 and S2 with various flowrate.

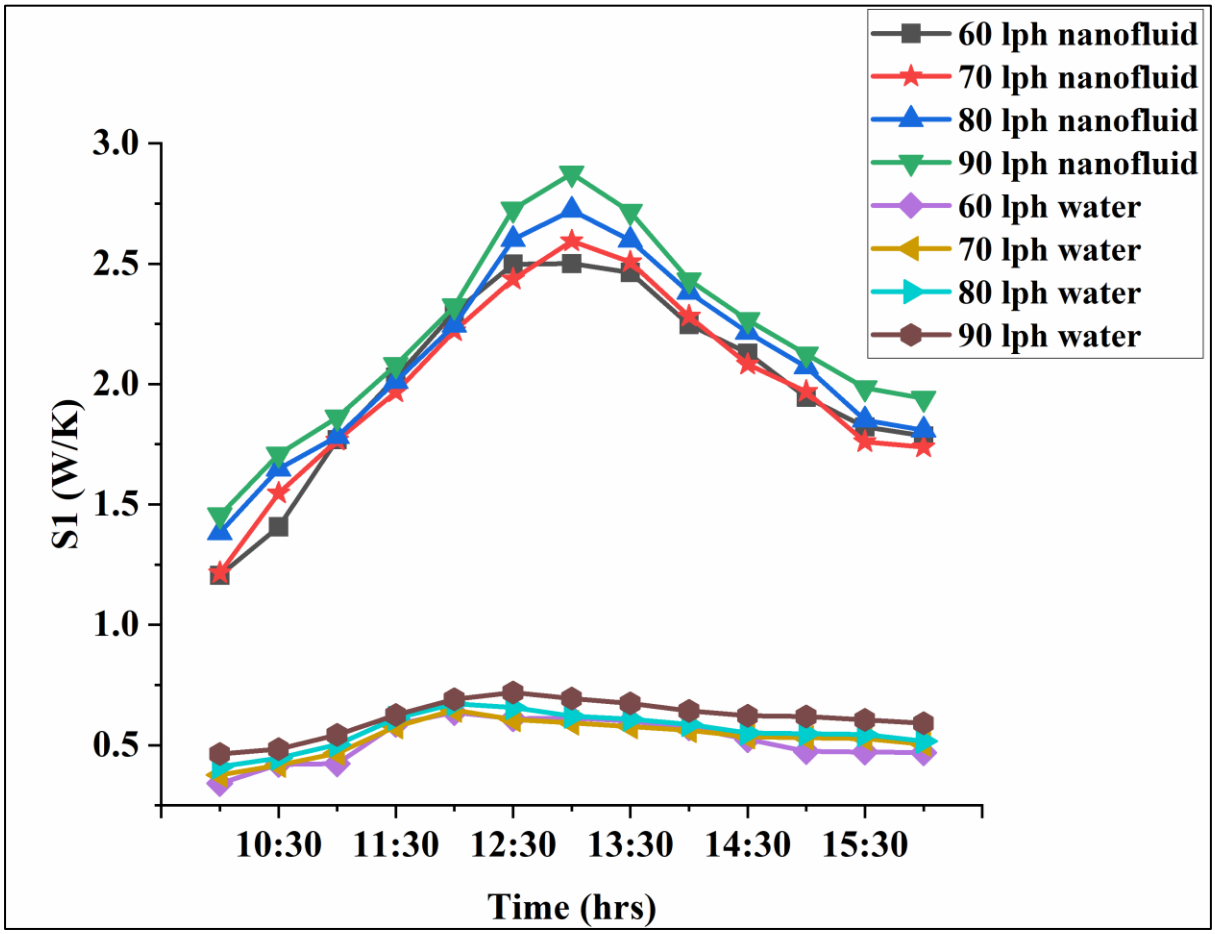

401

402 **Fig.10**: Instantaneous S1 of nanofluid and water at various flow rates.

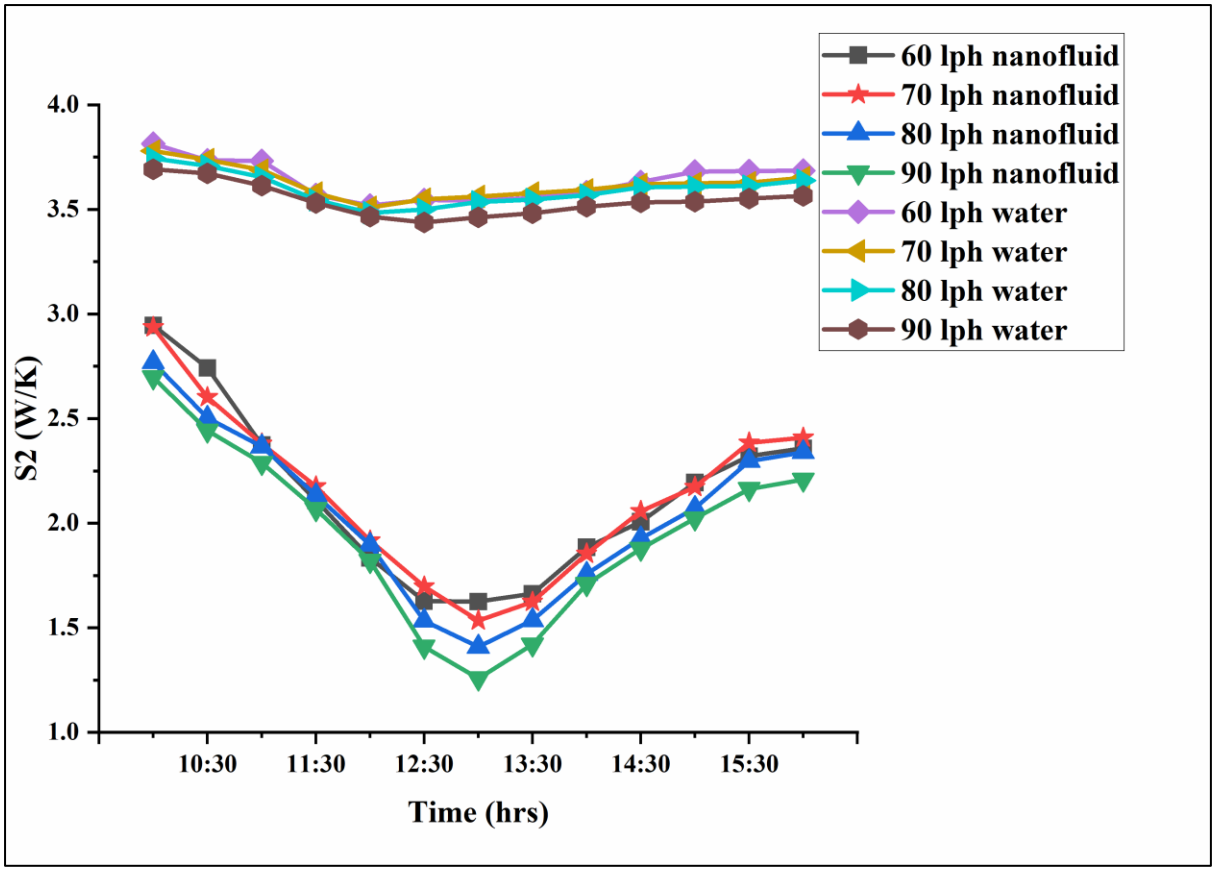

403

404 **Fig. 11**. Instantaneous S2 of nanofluid and water at various flow rates.

405

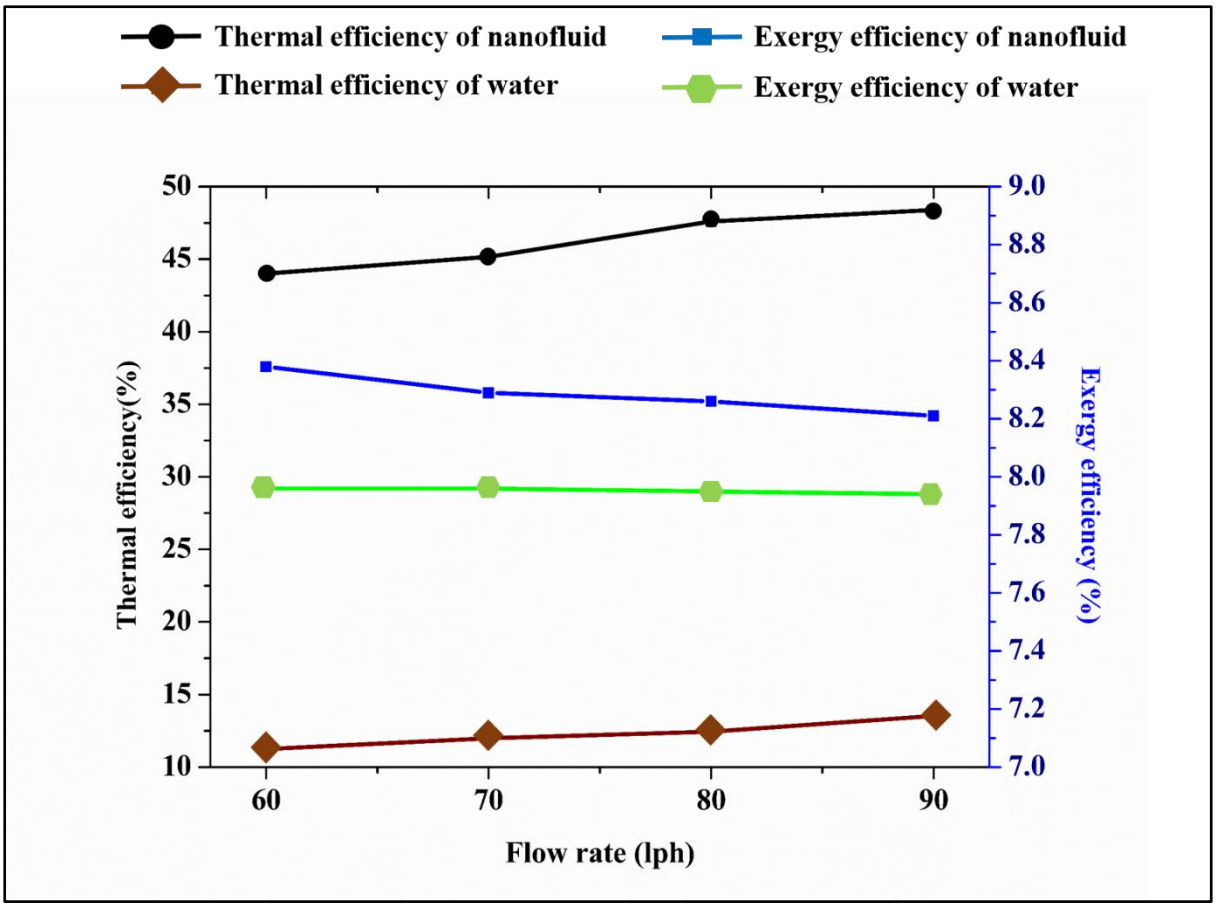

Fig. 12. Thermal efficiency and exergy efficiency at various flowrate.

Table. 5. Maximum temperature difference, thermal efficiency and exergy efficiency obtained for nanofluid and base fluid.

Flow rate (lph)	Temperature Difference (K)		Thermal Efficiency (%)		Exergy efficiency (%)	
	Base fluid	Nanofluid	Base fluid	Nanofluid	Base Fluid	Nanofluid
60	2.71	10.8	13.80	55.01	7.97	8.64
70	2.46	10.01	14.55	59.23	7.96	8.59
80	2.21	9.06	14.96	61.34	7.95	8.52
90	2.08	8.41	15.86	64.12	7.95	8.48

4. Conclusion

The study demonstrates the favourable influence of binary SiO_2/Ag-CuO nanofluid on augmenting the performance of volumetric absorption parabolic solar collector. The constituents in the nanofluid was optimised using the response surface methodology and desirability function. Nanofluid of optimum constituents (RTC of 1.234 and SRAF of

82.84%) was used as the working fluid in the volumetric absorption parabolic solar collector and the effect of flow rate on various performance parameters were estimated. The major findings are summarised as follows:

- A maximum temperature difference of 10.8K was observed for nanofluid at 60lph and 8.41K at 90 lph.
- SiO_2/Ag-CuO nanofluid improved the thermal performance of the collector with a maximum overall enhancement of 48.74% in thermal efficiency noted at a flow rate of 90lph.
- Increase in the flow rate leads to enhanced thermal efficiency of the collector, the maximum thermal efficiency of 55.01% and 64.12% were obtained at 60lph and 90lph.
- The presence of SiO_2/Ag-CuO nanofluid reduced the entropy generation and thus improved the exergy efficiency of the collector. However, entropy generation increased with the flow rate which in turn reduced the exergy efficiency.
- Exergy efficiency of collector using nanofluid was enhanced by 8.4% at 60 lph, in comparison with water.

REFERENCES

[1] Sanaz Akbarzadeh, Mohammad Sadegh Valipour, Heat transfer enhancement in parabolic trough collectors: A comprehensive review, Renew Sustain Energy Rev 92 (2018) 198–218 https://doi.org/10.1016/j.rser.2018.04.093

[2] R. Jain, R. Pitchumani, Fabrication and characterization of multiscale, fractal textured solar selective coatings, Sol. Energy Mater. Sol Cells 172 (2017) 213–219 https://doi.org/10.1016/j.solmat.2017.07.009

[3] G.C. Bakos, Ch. Tsechelidou Solar aided power generation of a 300 MW lignite fired power plant combined with line-focus parabolic trough collectors field, Renewable Energy 60 (2013) 540-547 https://doi.org/10.1016/j.renene.2013.05.024

[4] Jian-ping Meng, Xiao-peng Liu, Zhi-qiang Fu, Ke Zhang, Optical design of Cu/Zr0.2AlN0.8/ZrN/AlN/ZrN/AlN/Al34O62N4 solar selective absorbing coatings Sol. Energy 146 (2017) 430–435 https://doi.org/10.1016/j.solener.2017.03.012

[5] Xiaoxiao Yu, Yimin Xuan, Investigation on thermo-optical properties of CuO/Ag plasmonic nanofluids, Solar Energy 160 (2018) 200–207. https://doi.org/10.1016/j.solener.2017.12.007

[6] Tahereh B. Gorji, A.A. Ranjbar, A review on optical properties and application of nanofluids in direct absorption solar collectors (DASCs), Renew Sustain Energy Rev 72 (2017) 10–32 https://doi.org/10.1016/j.rser.2017.01.015

[7] Harriet Kimptona, Domenico Andrea Cristaldia, Eugen Stulzb, Xunli Zhang, Thermal performance and physicochemical stability of silver nanoprism based nanofluids for direct solar absorption, Sol. Energy 199 (2020) 366–376 https://doi.org/10.1016/j.solener.2020.02.039

[8] Shiva Gorjian, Hossein Ebadi , Francesco Calise , Ashish Shukla , Carlo Ingrao, A review on recent advancements in performance enhancement techniques for low-temperature solar collectors, Energy Convers. Manage 222 (2020) 113246 https://doi.org/10.1016/j.enconman.2020.113246

[9] Caiyan Qin, Joong Bae Kim, Bong Jae Lee, Performance analysis of a direct-absorption parabolic-trough solar collector using plasmonic nanofluids, Renewable Energy 143 (2019) 24-33 https://doi.org/10.1016/j.renene.2019.04.146

[10] Vishal Bhalla, Sachin Beejawat, Jay Doshi, Vikrant Khullar, Harjit Singh, Himanshu Tyagi, Silicone oil envelope for enhancing the performance of nanofluid based direct absorption solar collectors, Renewable Energy 145 (2020) 2733-2740 https://doi.org/10.1016/j.renene.2019.08.024

[11] Kongxiang Wang, Yan He, Pengyu Liu, Ankang Kan, Zhiheng Zheng, Lingling Wang, Huaqing Xie, Wei Yu, Highly-efficient nanofluid-based direct absorption solar collector enhanced by reverse-irradiation for medium temperature applications, Renewable Energy 159 (2020) 652-662 https://doi.org/10.1016/j.renene.2020.05.167

[12] Ahmet Z.Sahin, Mohammed Ayaz Uddin, Bekir S.Yilbas, AbdullahAl-Sharafi Performance enhancement of solar energy systems using nanofluids: An updated review, Renewable Energy 145 (2020) 1126-1148 https://doi.org/10.1016/j.renene.2019.06.108

[13] Sarkar J, Ghosh P, Adil A, A review on hybrid nanofluids: recent research, development and applications, Renew Sustain Energy Rev 43 (2015) 164–177 https://doi.org/10.1016/j.rser.2014.11.023

[14] Vishal Bhalla, Vikrant Khullar, Himanshu Tyagi, Experimental investigation of photo-thermal analysis of blended nanoparticles (Al_2O_3/Co_3O_4) for direct absorption solar thermal collector, Renewable Energy 123 (2018) 616-626 https://doi.org/10.1016/j.renene.2018.01.042

[15] Nan Chen, Haiyan Ma, Yang Li, Jinhu Cheng, Canying Zhang, Daxiong Wu, Haitao Zhu. Complementary optical absorption and enhanced solar thermal conversion of CuO-ATO nanofluids, Sol. Energy Mater. Sol Cells. 162 (2017) 83-92 https://doi.org/10.1016/j.solmat.2016.12.049

[16] Jia Zeng, Yimin Xuan, Enhanced solar thermal conversion and thermal conduction of MWCNT-SiO_2/Ag binary nanofluids, Appl. Energy, 212 (15) (2018), 809-819 https://doi.org/10.1016/j.apenergy.2017.12.083

[17] Pawel Keblinski, Jeffrey A. Eastman, David G. Cahill, Nanofluid for thermal transport, Mater. Today, 8 (6) (2005) 36-44 https://doi.org/10.1016/S1369-7021(05)70936-6

[18] Nor Azwadi Che Sidik, Muhammad Mahmud Jamil, Wan Mohd Arif Aziz Japar, Isa Muhammad Adamu, A review on preparation methods, stability and applications of hybrid nanofluids, Renew Sustain Energy Rev 80 (2017) 1112-1122 https://doi.org/10.1016/j.rser.2017.05.221

[19] Mikko Makela, Experimental design and response surface methodology in energy applications: A tutorial review, Energy Convers. Manage, 151 (2017) 630-640. https://doi.org/10.1016/j.enconman.2017.09.021

[20] Wenlian Ye, Peng Yang, Yingwen Liu, Multi-objective thermodynamic optimization of a free piston Stirling engine using response surface methodology, Energy Convers. Manage 176 (2018) 147–163
https://doi.org/10.1016/j.enconman.2018.09.011

[21] Sreehari Sreekumar, Albin Joseph, C.S. Sujith Kumar, Shijo Thomas, Investigation on influence of antimony tin oxide/silver nanofluid on direct absorption parabolic solar collector, J. Clean. Prod. 249 (2019) 119378
https://doi.org/10.1016/j.jclepro.2019.119378

[22] A. Kasaeian, S. Daviran, R. D. Azarian, A. Rashidi, 2015, Performance evaluation and nanofluid using capability study of a solar parabolic trough collector, J. Clean. Prod. 89 (2015) 368–375.
https://doi.org/10.1016/j.enconman.2014.09.056.

[23] E. Bellos, C. Tzivanidis, Thermal analysis of parabolic trough collector operating with mono and hybrid nanofluids, Sustain. Energy Technol. Assess. 26 (2018) 105-115.
https://doi.org/10.1016/j.seta.2017.10.005

[24] T.P. Otanicar, P.E. Phelan, J. S. Golden, Optical properties of liquids for direct absorption solar thermal energy systems, Sol. Energy 83 (2009) 969–977.
https://doi.org/ 10.1016/j.solener.2008.12.009.

[25] Yong Yang Gan, Hwai Chyuan Ong, Tau Chuan Ling, N.W.M. Zulkifli, Chin-Tsan Wang, Yung-Chin Yang, Thermal conductivity optimization and entropy generation analysis of titanium dioxide nanofluid in evacuated tube solar collector, Appl. Therm. Eng. 145 (2018) 155–164.
https://doi.org/10.1016/j.applthermaleng.2018.09.012

[26] Moffat, R.J., 1985. Describing the uncertainties in the experimental results. Exp. Therm. Fluid Sci. 1, 3-17.
https://doi.org/10.1016/0894-1777(88)90043-X.

[27] Salma Parvin, Rehena Nasrin, M.A. Alim, Heat transfer and entropy generation through nanofluid filled direct absorption solar collector, Int. J. Heat Mass Transfer 71 (2014) 386–395.
http://dx.doi.org/10.1016/j.ijheatmasstransfer.2013.12.043

[28] Albin Joseph, Sreehari Sreekumar, C S Sujith kumar, Shijo Thomas, Optimisation of thermo-optical properties of SiO_2/Ag-CuO nanofluid for direct absorption solar collectors, J. Mol. Liq. (2019) 111986.
https://doi.org/10.1016/j.molliq.2019.111986

[29] T. Aguilar, E. Sani, L. Mercatelli, I. Carrillo-Berdugo, E. Torres, J. Navas, Exfoliated graphene oxide-based nanofluids with enhanced thermal and optical properties for solar collectors in concentrating solar power, J. Mol. Liq 306 (2020) 112682.
https://doi.org/10.1016/j.molliq.2020.112862

[30] Omid Mahian, Ali Kianifar, Soteris A. Kalogirou, Ioan Pop, Somchai Wongwises, A review of the applications of nanofluids in solar energy, Int. J. Heat Mass Transfer 57 (2013) 582–594
http://dx.doi.org/10.1016/j.ijheatmasstransfer.2012.10.037

[31] M.M. Heyhat, M. Valizade, Sh. Abdolahzade, M. Maerefat, Thermal efficiency enhancement of direct absorption parabolic trough solar collector (DAPTSC) by using nanofluid and metal foam, Energy 192 (2020) 116662
https://doi.org/10.1016/j.energy.2019.116662

[32] M.A. Sharafeldin, Gyula Grof, Evacuated tube solar collector performance using

CeO2/water, nanofluid, J. Clean. Prod 185 (2018) 347-356
https://doi.org/10.1016/j.jclepro.2018.03.054

433

*Declaration of Interest Statement

Conflicts of interest

The authors hereby declare that there has no conflict of interest

***Credit Author Statement**

Author contributions

Use this form to specify the contribution of each author of your manuscript. A distinction is made between five types of contributions: Conceived and designed the analysis; Collected the data; Contributed data or analysis tools; Performed the analysis; Wrote the paper.

For each author of your manuscript, please indicate the types of contributions the author has made. An author may have made more than one type of contribution. Optionally, for each contribution type, you may specify the contribution of an author in more detail by providing a one-sentence statement in which the contribution is summarized. In the case of an author who contributed to performing the analysis, the author's contribution for instance could be specified in more detail as 'Performed the computer simulations', 'Performed the statistical analysis', or 'Performed the text mining analysis'.

If an author has made a contribution that is not covered by the five pre-defined contribution types, then please choose 'Other contribution' and provide a one-sentence statement summarizing the author's contribution.

Manuscript title: Energy and Exergy analysis of SiO2/Ag-CuO plasmonic nanofluid on direct absorption parabolic solar collector

Author 1: Albin Joseph

☒ Conceived and designed the analysis
Specify contribution in more detail (optional; no more than one sentence)

☒ Collected the data
Specify contribution in more detail (optional; no more than one sentence)

☒ Contributed data or analysis tools
Specify contribution in more detail (optional; no more than one sentence)

☒ Performed the analysis
Specify contribution in more detail (optional; no more than one sentence)

☒ Wrote the paper
Specify contribution in more detail (optional; no more than one sentence)

☐ Other contribution
Specify contribution in more detail (required; no more than one sentence)

Author 2: Sreehari Sreekumar

☒ Conceived and designed the analysis
Specify contribution in more detail (optional; no more than one sentence)

☒ Collected the data
Specify contribution in more detail (optional; no more than one sentence)

☒ Contributed data or analysis tools
Specify contribution in more detail (optional; no more than one sentence)

☐ Performed the analysis
Specify contribution in more detail (optional; no more than one sentence)

☐ Wrote the paper
Specify contribution in more detail (optional; no more than one sentence)

☐ Other contribution
Specify contribution in more detail (required; no more than one sentence)

Author 3: Shijo Thomas

☒ Conceived and designed the analysis
Specify contribution in more detail (optional; no more than one sentence)

☐ Collected the data
Specify contribution in more detail (optional; no more than one sentence)

☒ Contributed data or analysis tools
Specify contribution in more detail (optional; no more than one sentence)

☒ Performed the analysis
Specify contribution in more detail (optional; no more than one sentence)

☒ Wrote the paper
Specify contribution in more detail (optional; no more than one sentence)

☐ Other contribution
Specify contribution in more detail (required; no more than one sentence)

Author 4: Enter author name

☐ Conceived and designed the analysis
Specify contribution in more detail (optional; no more than one sentence)

☐ Collected the data
Specify contribution in more detail (optional; no more than one sentence)

☐ Contributed data or analysis tools
Specify contribution in more detail (optional; no more than one sentence)

☐ Performed the analysis
Specify contribution in more detail (optional; no more than one sentence)

☐ Wrote the paper
Specify contribution in more detail (optional; no more than one sentence)

☐ Other contribution
Specify contribution in more detail (required; no more than one sentence)

Author 5: Enter author name

☐ Conceived and designed the analysis
Specify contribution in more detail (optional; no more than one sentence)

☐ Collected the data
Specify contribution in more detail (optional; no more than one sentence)

☐ Contributed data or analysis tools
Specify contribution in more detail (optional; no more than one sentence)

☐ Performed the analysis
Specify contribution in more detail (optional; no more than one sentence)

☐ Wrote the paper
Specify contribution in more detail (optional; no more than one sentence)

☐ Other contribution
Specify contribution in more detail (required; no more than one sentence)

Author 6: Enter author name

☐ Conceived and designed the analysis
Specify contribution in more detail (optional; no more than one sentence)

☐ Collected the data
Specify contribution in more detail (optional; no more than one sentence)

☐ Contributed data or analysis tools
Specify contribution in more detail (optional; no more than one sentence)

☐ Performed the analysis
Specify contribution in more detail (optional; no more than one sentence)

☐ Wrote the paper
Specify contribution in more detail (optional; no more than one sentence)

☐ Other contribution
Specify contribution in more detail (required; no more than one sentence)

Author 7: Enter author name

☐ Conceived and designed the analysis
Specify contribution in more detail (optional; no more than one sentence)

☐ Collected the data
Specify contribution in more detail (optional; no more than one sentence)

☐ Contributed data or analysis tools
Specify contribution in more detail (optional; no more than one sentence)

☐ Performed the analysis
Specify contribution in more detail (optional; no more than one sentence)

☐ Wrote the paper
Specify contribution in more detail (optional; no more than one sentence)

☐ Other contribution
Specify contribution in more detail (required; no more than one sentence)

Author 8: Enter author name

☐ Conceived and designed the analysis
Specify contribution in more detail (optional; no more than one sentence)

☐ Collected the data
Specify contribution in more detail (optional; no more than one sentence)

☐ Contributed data or analysis tools
Specify contribution in more detail (optional; no more than one sentence)

☐ Performed the analysis
Specify contribution in more detail (optional; no more than one sentence)

☐ Wrote the paper
Specify contribution in more detail (optional; no more than one sentence)

☐ Other contribution
Specify contribution in more detail (required; no more than one sentence)

Author 9: Enter author name

☐ Conceived and designed the analysis
Specify contribution in more detail (optional; no more than one sentence)

☐ Collected the data
Specify contribution in more detail (optional; no more than one sentence)

☐ Contributed data or analysis tools
Specify contribution in more detail (optional; no more than one sentence)

☐ Performed the analysis
Specify contribution in more detail (optional; no more than one sentence)

☐ Wrote the paper
Specify contribution in more detail (optional; no more than one sentence)

☐ Other contribution
Specify contribution in more detail (required; no more than one sentence)

Author 10: Enter author name

☐ Conceived and designed the analysis
Specify contribution in more detail (optional; no more than one sentence)

☐ Collected the data
Specify contribution in more detail (optional; no more than one sentence)

☐ Contributed data or analysis tools
Specify contribution in more detail (optional; no more than one sentence)

☐ Performed the analysis
Specify contribution in more detail (optional; no more than one sentence)

☐ Wrote the paper
Specify contribution in more detail (optional; no more than one sentence)

☐ Other contribution
Specify contribution in more detail (required; no more than one sentence)